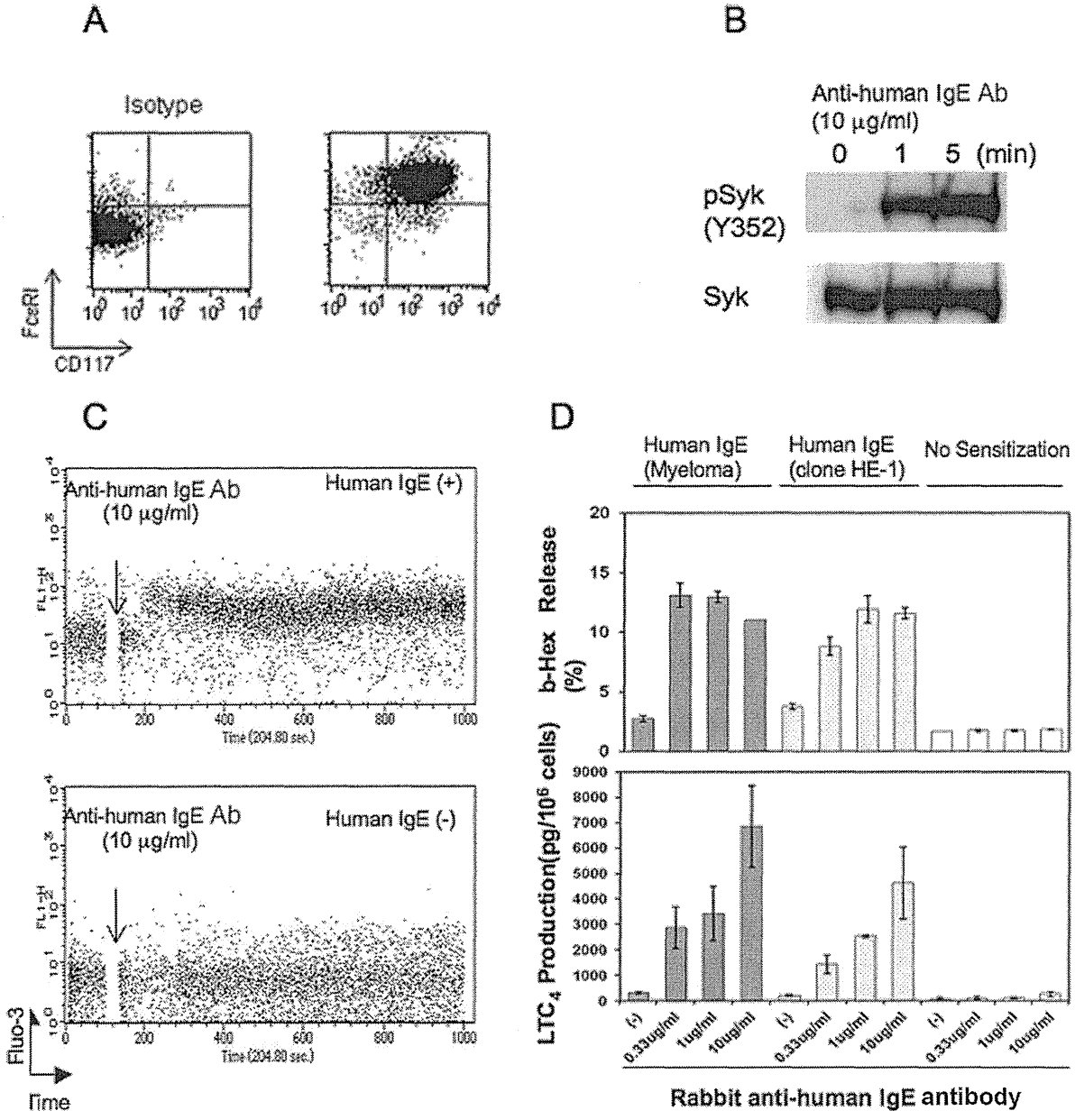

Fig. 2. Functional MCs developed *in vitro*. (A) The DP cells were cultured in the presence of mouse SCF for 10 weeks, incubated with hybridoma-derived human IgE (HE-1) overnight and processed for flow cytometry as described in Methods. (B) Marmoset MCs sensitized with human IgE (HE-1) were stimulated with rabbit anti-human IgE polyclonal antibody (10 μg/ml) for the indicated times. The total cell lysates were analyzed by immunoblotting with anti-phospho Syk (Tyr352) antibody. The blot was reprobed with anti-non-phospho Syk antibody. (C) Calcium mobilization in the human IgE (HE-1)-sensitized and unsensitized MCs. Changes in Fluo3 fluorescence were determined by employing flow cytometry after loading of rabbit anti-human IgE polyclonal antibody (10 μg/ml). (D) Marmoset MCs can degranulate and release LTC_4 in response to FcεRI stimulation. Marmoset MCs were sensitized with myeloma-derived human IgE or hybridoma-derived human IgE (HE-1) overnight. The IgE-sensitized MCs were stimulated with rabbit anti-human IgE polyclonal antibody at the indicated concentrations for 30min. Degranulation response was determined by β-hexosaminidase release (upper panel). LTC_4 production was analyzed with an LTC_4 EIA kit (bottom panel).

cells with both anti-CD117 mAb and human IgE. Almost all of $CD117^+$ cells expressed FcεR, confirming that the cells are MCs (Fig. 3A, right panel). In addition, because marmoset spleen itself contained only a small (3.4%) population of $CD34^-CD117^+$, NOG mice appear to provide favorable conditions for progenitors to expand and differentiate into MCs.

As shown in Fig. 3B, the percentage of $CD34^-CD117^+$ population in spleens was higher in DP-NOG mice (15% on

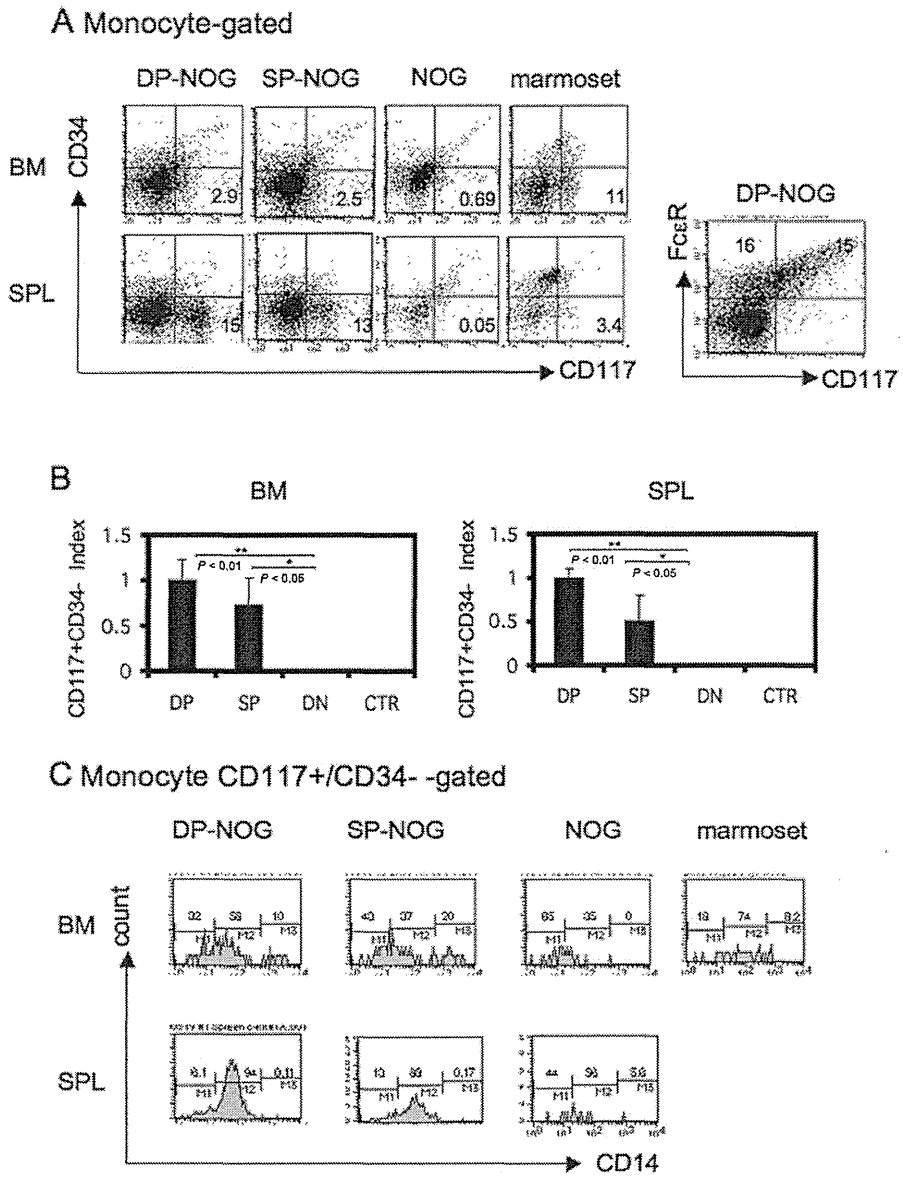

Fig. 3. Expression of MC markers in marmoset cells that were developed in NOG mice. CD117$^+$CD34$^+$ (DP) and CD117$^+$CD34$^-$ (SP) cells were prepared from marmoset bone marrow and transplanted into NOG mice. After 4 weeks, bone marrow cells (BM) and splenocytes (SPL) were taken from mice and processed for flow cytometry with anti-marmoset CD45, anti-marmoset CD34, anti-marmoset CD117, anti-human CD14 mAbs and human IgE/anti-human IgE mAbs. (A) The monocyte-gated fractions are displayed for the CD34 and CD117 expression (left panels). Cells from nontransplanted NOG mice and those from marmoset served as controls. The numbers indicate the percentages of CD34$^-$CD117$^+$ subfraction. Right panel shows the DP-NOG spleen cells stained with CD117 and human IgE. (B) Mean ± SD were calculated and expressed as index for the percentages of CD34$^-$CD117$^+$ subfractions from three independent experiments (n = 3) as in (A). Control (CTR) means cells from nontransplanted NOG mice. Statistically significant differences were detected between DP and SP in spleen ($P < 0.05$). (C) The monocyte/CD45$^+$CD117$^+$CD34$^-$-gated fractions are displayed for their CD14 expressions. The numbers indicate the percentages of CD14^{lo}, CD14^{int} and CD14^{hi} subfractions, respectively.

average, equalized to index 1.0) compared with SP-NOG mice (7% on average, equalized to index 0.5). This 2-fold difference was statistically significant ($P < 0.05$). The cell number of CD34$^-$CD117$^+$ population in NOG spleen showed around 1 × 10^5 to 2 × 10^5 in DP-NOG and 0.5 × 10^5 in DP-NOG and the pattern was very similar to that of the cell ratio (Supplementary Figure S2 is available at *International Immunology* Online). In the case of bone marrow, percentages of CD34$^-$CD117$^+$ population were as low as 2–3%, but DP-NOG mice generated a slightly higher level of this population compared with SP-NOG mice. This suggests that the DP fraction likely contains more MC progenitors than the SP fraction, a notion

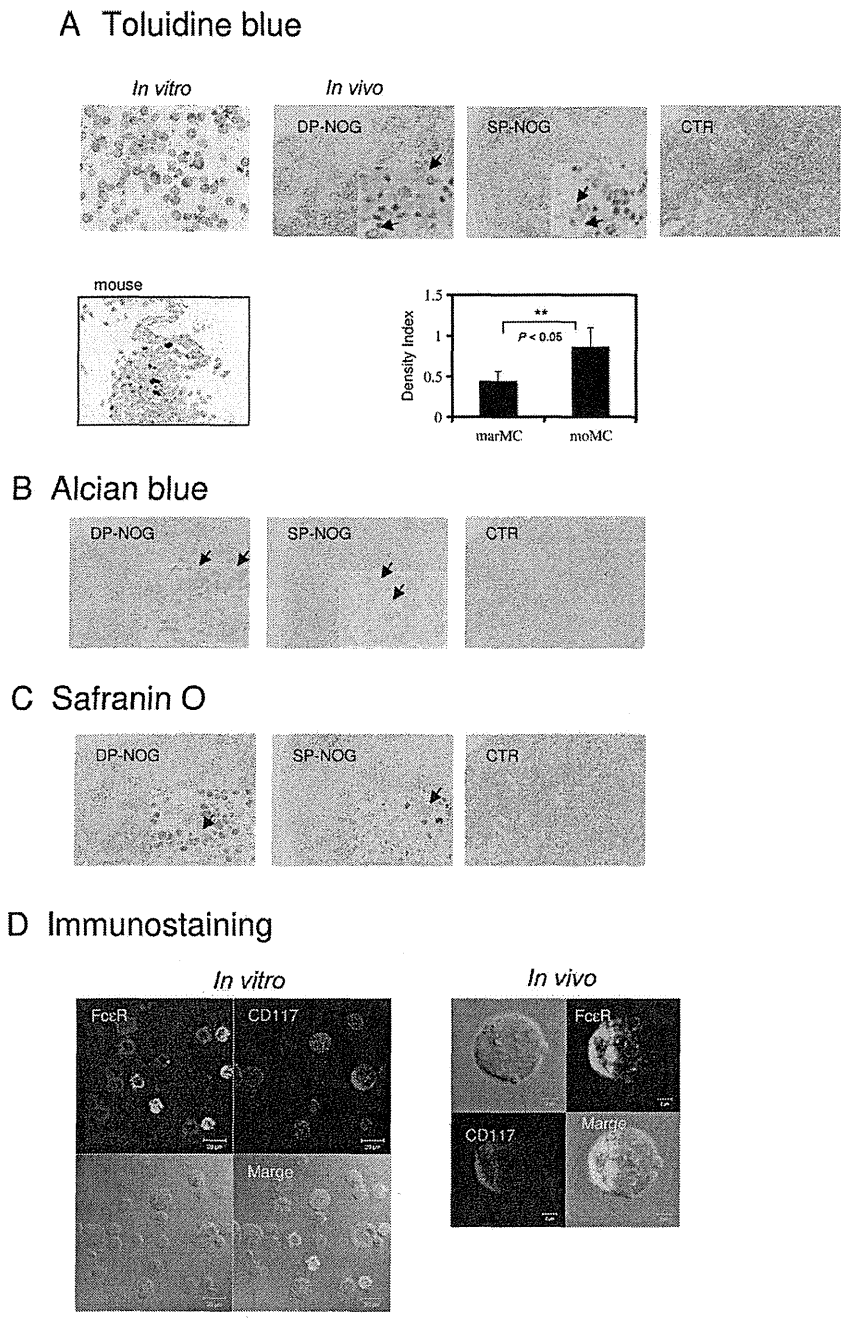

Fig. 4. Histochemical analyses of marmoset cells expanded *in vitro* and in transplanted NOG mice. (A) Toluidine blue staining of cells. Top left: $CD117^{+}CD34^{+}$ (DP) cells prepared from marmoset bone marrow were cultured *in vitro* in the presence of mouse SCF for 4 weeks, fixed and stained with toluidine blue. Top middle: $CD117^{+}CD34^{+}$ (DP) and $CD117^{+}CD34^{-}$ (SP) fractions of marmoset bone marrow cells were transplanted into NOG mice. After 4 weeks, spleens were taken and their sections were stained. Arrowheads indicate the metachromatically stained cells. Top right: Control (CTR) means a spleen from nontransplanted mouse. Bottom left: A section of mouse spleen was stained. Bottom right: Histograms represent the relative densities of metachromatically stained granules in MCs detected in spleens of marmoset cell-transplanted (marMC; $n = 69$) or nontransplanted NOG (moMC; $n = 8$) mice. A statistically significant difference was detected between the two samples ($P < 0.05$). (B) Alcian blue and (C) safranin O staining of spleen sections prepared as in (A). Arrowheads indicate metachromatically stained cells. (D) Confocal microscopy of *in vitro*- and *in vivo*-developed mast cells. BM cells cultured with SCF for 4 weeks (left panels) and sorted CD117 SP cells from DP-transplanted NOG spleen were stained for human FcεR (Alexa488-labeled) and CD117 (PE-labeled). FcεR (Green) and CD117 (Red) double expression is shown in small granule-positive cells. Most CD117 SP cells were small human IgE-positive cells and included granules in the cytoplasm.

in line with the results obtained by *in vitro* culture experiments (Fig. 1). In addition, MC differentiation was observed more prominently in spleen than in bone marrow of NOG mice.

To further characterize the nature of MCs, the monocyte/CD34$^-$CD117$^+$-gated fraction was then examined for the expression of CD14 (Fig. 3C). CD14 expression is known to be absent in progenitors, be induced in myeloid–monocyte lineage *in vitro* and then decline again to a background level in mature MCs in humans (27). In bone marrow, and more clearly in splenocytes, a CD14^{int} subfraction was detected. Thus, in transplanted NOG mice, the DP and SP fractions of marmoset bone marrow cells tended to differentiate into a MC lineage at least up to an immature stage.

Histochemical staining revealed development of marmoset MCs in transplanted NOG mice

Heparin-containing granules present in the cytoplasm of MCs were stained metachromatically by toluidine blue dye. Marmoset bone marrow cells cultured *in vitro* in the presence of SCF were stained by this dye (Fig. 4A, top). In addition to normochromatically stained cells (blue), metachromatically stained cells (red-purple) were identified. This observation further supports the concept of the differentiation of MCs from marmoset bone marrow cells. Histological sections of spleens were prepared from marmoset cell-transplanted NOG mice and processed for toluidine blue staining (Fig. 4A, middle). In both DP- and SP-transplanted spleens, metachromatically stained cells were detected, indicating the development of MCs *in vivo* as well.

We noticed that the extent of metachromatic staining was relatively mild in DP-transplanted spleen MCs (n = 69; Fig. 4A, middle) compared with that in nontransplanted spleen MCs (n = 8; Fig. 4A, bottom). Then, we measured the density of dye deposition on granules by densitometer, calculating it as density index. MCs of mouse origin were significantly heavily stained compared with marmoset MCs ($P < 0.05$). The differential staining patterns by toluidine blue might have reflected some qualitative/quantitative differences in the contents of heparin-containing granules in MCs of these two species.

Developing MCs are known to be distributed into distinct parts of the body and further differentiate into tissue-residing and/or mucosa-residing subtypes. To distinguish the subtypes of MCs developing in transplanted NOG mice, spleen sections were stained by another set of dyes (Fig. 4B and 4C). In both DP- and SP-transplanted spleens, cells were also metachromatically stained not only by alcian blue but also by safranin O. These results suggest that a substantial portion of marmoset MCs developing in transplanted NOG spleens might correspond to the tissue type (characterized by metachromasy for toluidine blue, alcian blue and safranin O) but does not exclude the possible coexistence of mucosa-type MCs (characterized by metachromasy for toluidine blue and alcian blue but not for safranin O).

Finally, we purified the spleen CD117SP cells and stained them with FcεR. Confocal microscopy revealed that the CD117SP cells were FcεR-positive and includes many granules, suggesting them to be MCs (Fig. 4D, right panels). Compared with *in vitro*-developed cell populations (4 weeks) in which CD117$^+$FcεR$^-$ progenitor cells were observed, FcεR-expressing small cells simultaneously expressed CD117 although the level was not high (Fig. 4D, left panels). FcεRI cross-linking with avidine-conjugated secondary antibody induced degranulation of the cells.

Marmoset MCs developed in NOG spleen is functional

Chymase and tryptase are signature proteases of MCs. Chymase 1 is expressed only in tissue-type MCs, whereas tryptase β2 expression is detected in both tissue and mucosa types of MCs. Using information available from a draft genome of *C. jacchus* from the UCSC genome browser, primers were designed to detect chymase 1 and tryptase β2 transcripts. Authenticity of PCR-amplified sequences using these primers was confirmed (data not shown).

We prepared RNAs from *in vitro* cultures and *in vivo*-transplanted spleens and processed them for RT–PCR analyses (Fig. 5A). Both chymase 1 and tryptase β2 transcripts were detected in the cultures of DP and SP marmoset bone marrow cells although the band density of tryptase β2 was

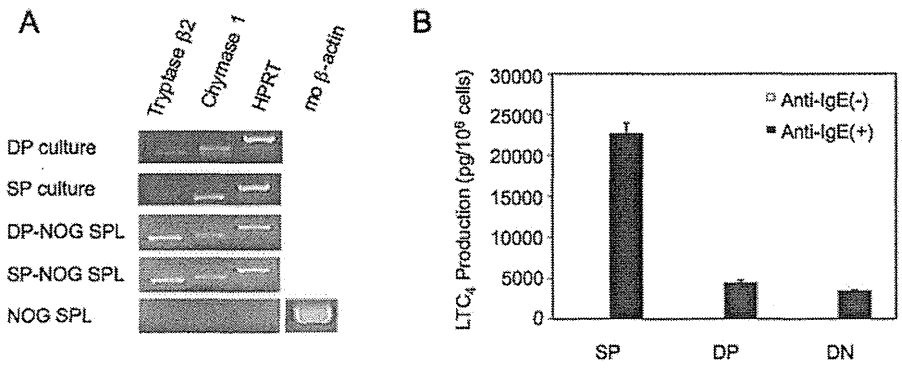

Fig. 5. Functional analysis of CB-NOG-derived MCs. (A) RT–PCR analyses of transcripts encoding MC. RNA was prepared from the indicated samples including the cultures of CD117$^+$CD34$^+$ (DP) or CD117$^+$CD34$^-$ (SP) cells, spleens of DP- or SP-transplanted or nontransplanted NOG mice or bone marrow or spleens of common marmoset. Transcripts of MC proteases were examined. Hypoxanthine phosphoribosyl transferase (*HPRT*) served as a control. (B) The SP (MC), DP and DN fractions were sorted out and IgE sensitized overnight. After that they were stimulated with rabbit anti-human IgE polyclonal antibody at 10 μg/ml for 30 min. LTC_4 production was analyzed with an LTC_4 EIA kit (n = 3).

relatively low. In addition, both transcripts were also observed in spleens of DP- and SP-transplanted NOG mice, whereas corresponding transcripts were not found at all in nontransplanted NOG mice, indicating the origin of chymase 1 and tryptase β2 transcripts to be from transplanted and expanding marmoset cells. These results support the notion that the CD117$^+$ cells found in *in vitro* cultures and *in vivo*-transplanted spleens indeed represented MCs and also that at least a portion of the population contained tissue-type MCs.

Next, *in vivo*-developed MCs were sorted out, sensitized with human IgE and stimulated by cross-linking the FcεR-bound IgE molecule with anti-human IgE antibody. LTC_4 was significantly produced by CD117SP compared with other fractions (Fig. 5B). These results suggest that CB-NOG-developed MCs are at least partially functional MCs.

Discussion

The initial trial to identify hematopoietic progenitors in the common marmoset was reported by Izawa *et al.* in 2004 (28). They developed an anti-marmoset CD34 mAb, isolated CD34$^+$ cells from marmoset bone marrow and transplanted them into immunodeficient NOD-SCID mice. Four weeks after transplantation, CD11b$^+$CD14$^+$ cells appeared in the peripheral blood of mice, and their origin was judged to be marmoset because of their cross-reactivity to anti-human CD11b and CD14 mAbs (29). This result demonstrated the differentiation potential of marmoset CD34$^+$ cells to myeloid lineage. Subsequently, our group established anti-marmoset CD117 and CD45 mAbs and fractionated marmoset bone marrow cells into four subfractions based on the expression of CD34 and CD117 (25). We showed that the CD34$^+$CD117$^+$ DP fraction contained differentiation activity to multiple hematopoietic lineages in colony-forming assays. In the present study, we extended the analysis of marmoset hematopoietic progenitors to MC differentiation by utilizing anti-marmoset-specific mAbs.

According to extensive studies on hematopoiesis in humans, CD34$^+$CD117^{lo} cells turn out to represent hematopoietic stem cells (30–34), whereas CD34$^+$CD117^{hi} cells contain myeloid progenitor activity that can develop lineages of MCs and monocytes (32). Upon differentiation, mature MCs exhibit the following characteristics in surface marker expression: (i) CD34$^-$CD117$^+$ (NB, mature monocytes are CD34$^-$CD117$^-$), (ii) FcεRI$^+$ (NB, basophils are FcεRI$^+$CD117$^-$), (iii) CD45$^+$ (NB, all leukocyte lineages including MCs are CD45$^+$) and (iv) CD13$^-$CD14$^-$ (NB, hematopoietic stem cells are also CD13$^-$CD14$^-$, but myeloid progenitors including MC progenitors become CD13^{int}CD14^{int}. Then, mature MCs return to CD13$^-$CD14$^-$ again, whereas mature monocytes transit to CD13^{hi}CD14^{hi}). We prepared DP cells from marmoset bone marrow and subjected them to both *in vitro* culture in the presence of SCF and *in vivo* transplantation assays into NOG mice. *In vitro* we could detect the appearance of cells with CD34$^-$CD117$^+$ and FcεRI$^+$ (thus capable of binding human IgE), and *in vivo* we demonstrated the emergence of cells with CD34$^-$CD117$^+$. These cells also expressed CD45 (data not shown). These are indeed indications of authentic MC differentiation. In the developed MCs, Syk was tyrosine phosphorylated and the Ca^{2+} influx was observed after the FcεR cross-linking. They released LTC_4 and β-hexosaminidase simultaneously. The results confirmed that the MCs were functional MCs. A particularly important finding was that the differentiation activity to MC lineage was detected at a significantly higher rate in the DP fraction compared with the SP fraction (no such activity in the DN fraction). This tendency was true for both *in vitro* and *in vivo* assays. The exact differentiation pathway along the MC lineage is not known in terms of the DP and SP fractions (15,35). It is also not clear whether the CD34$^-$CD117$^+$CD45$^+$CD14^{int} fraction detected *in vivo* corresponds to myeloid progenitors and/or immature MCs. In any case, because we could demonstrate differentiation of the DP fraction to MC lineage, we can label the progenitor cells with green fluorescent protein (GFP), transplant them into syngenic marmoset and monitor the pathway of MC development *in vivo*. For this purpose, marmoset cells might be useful as a good model or control to mimic human MCs.

In mice (and humans), mature MCs are categorized into tissue and mucosa types, depending on their site of residence (36). The two types can be distinguished from each other by histochemical staining patterns with dyes and by differential expression patterns of proteases. Firstly, tissue-type MCs contain heparin-positive granules and are stained metachromatically by toluidine blue, alcian blue and safranin O. On the other hand, mucosa-type MCs, which possess chondroitin sulfate-positive granules, are stained metachromatically by toluidine blue and alcian blue but not safranin O. To be noted as a complicated situation is the mucosa type of human MCs, which are reported to contain both chondroitin sulfate and heparin. In our analyses of marmoset cell-transplanted NOG mice, we could find metachromatically stained MCs. They were stained by all three dyes, suggesting the differentiated MCs to be a tissue type. Secondly, tissue-type MCs express both tryptase and chymase, whereas mucosa-type MCs express only tryptase. We could detect both transcripts of tryptase β2 and chymase 1 in *in vitro*-cultured and *in vivo*-transplanted marmoset cells. This again indicates the existence of tissue-type MCs. Thus, although identification of mucosa-type MCs remains ambiguous, DP cells from marmoset bone marrow were shown to have the potential to differentiate at least into tissue-type MCs based on dye-staining and protease expression profiles. It must be noted that the density of toluidine blue-stained granules was significantly lower in marmoset MCs (suggesting a smaller amount of heparin content) compared with those in mouse MCs.

In spleen sections of marmoset and NOG mice, morphologically diagnosed MCs are detected only scarcely (data not shown). Also, in mononuclear cells of peripheral blood and splenocytes prepared from marmoset or NOG mice, a transcript encoding *IL-4* is barely detected (25). In contrast, we found substantial numbers of differentiated MCs and an enhanced level of *IL-4* transcript in spleens of NOG mice transplanted with marmoset DP cells (data not shown). Also, in the case of spleens of NOG mice transplanted with human hematopoietic progenitors, development of tissue-type MCs has been reported (24). Therefore, xenotransplantation (transfer of marmoset DP cells or human hematopoietic progenitors into mouse) might somehow provide an environment favorable for MC differentiation in spleens of NOG mice. As a subject for future research, candidate molecule(s) involved in such an environmental modification must be explored. Particularly interesting might be the possible contribution of cytokines including IL-4.

It remains to be determined to what extent marmoset MCs developing in NOG mice can mimic human MCs. Models of type I allergy such as pollinosis have been established in rodents but not in nonhuman primates. As the common marmoset immune system is more akin to human than mouse, it would be better to establish an allergy model of nonhuman primate like the common marmoset. Expansion and characterization of marmoset MCs in transplanted NOG mice may contribute to a novel model for understanding the pathogenesis of human allergic diseases.

Supplementary data

Supplementary data are available at *International Immunology* Online.

Funding

Grant-in-Aid for Scientific Research (KAKENHI) (C) (22500391); MEXT-Supported Program for the Strategic Research Foundation at Private Universities (2012–202016); 2010 Tokai University School of Medicine Research Aid (to S.S.).

Acknowledgements

The authors thank Dr Johbu Itoh, Dr Yoshinori Okada (Teaching and Research Support Center, Tokai University School of Medicine) and Miyuki Kuronuma (Central Institute for Experimental Animals) for their technical assistance and suggestions.

References

1 Galli, S. J., Grimbaldeston, M. and Tsai, M. 2008. Immunomodulatory mast cells: negative, as well as positive, regulators of innate and acquired immunity. *Nat. Rev. Immunol.* 8:478.
2 Galli, S. J. and Tsai, M. 2010. Mast cells in allergy and infection: versatile effector and regulatory cells in innate and adaptive immunity. *Eur. J. Immunol.* 40:1843.
3 Kim, H. Y., DeKruyff, R. H. and Umetsu, D. T. 2010. The many paths to asthma: phenotype shaped by innate and adaptive immunity. *Nat. Immunol.* 11:577.
4 Kalesnikoff, J. and Galli, S. J. 2010. Anaphylaxis: mechanisms of mast cell activation. *Chem. Immunol. Allergy* 95:45.
5 Finkelman, F. D., Hogan, S. P., Hershey, G. K., Rothenberg, M. E. and Wills-Karp, M. 2010. Importance of cytokines in murine allergic airway disease and human asthma. *J. Immunol.* 184:1663.
6 Kawakami, T., Ando, T., Kimura, M., Wilson, B. S. and Kawakami, Y. 2009. Mast cells in atopic dermatitis. *Curr. Opin. Immunol.* 21:666.
7 Mestas, J. and Hughes, C. C. 2004. Of mice and not men: differences between mouse and human immunology. *J. Immunol.* 172:2731.
8 Oboki, K., Ohno, T., Saito, H. and Nakae, S. 2008. Th17 and allergy. *Allergol. Int.* 57:121.
9 Shik, D. and Munitz, A. 2010. Regulation of allergic inflammatory responses by inhibitory receptors. *Clin. Exp. Allergy.* 40:700.
10 Kirshenbaum, A. S., Goff, J. P., Semere, T., Foster, B., Scott, L. M. and Metcalfe, D. D. 1999. Demonstration that human mast cells arise from a progenitor cell population that is CD34(+), c-kit(+), and expresses aminopeptidase N (CD13). *Blood* 94:2333.
11 Yoshikubo, T., Inoue, T., Noguchi, M. and Okabe, H. 2006. Differentiation and maintenance of mast cells from CD34(+) human cord blood cells. *Exp. Hematol.* 34:320.
12 Rao, K. N. and Brown, M. A. 2008. Mast cells: multifaceted immune cells with diverse roles in health and disease. *Ann. NY Acad. Sci.* 1143:83.
13 Abraham, S. N. and St John, A. L. 2010. Mast cell-orchestrated immunity to pathogens. *Nat. Rev. Immunol.* 10:440.
14 Kumar, V. and Sharma, A. 2010. Mast cells: emerging sentinel innate immune cells with diverse role in immunity. *Mol. Immunol.* 48:14.
15 Arinobu, Y., Iwasaki, H. and Akashi, K. 2009. Origin of basophils and mast cells. *Allergol. Int.* 58:21.
16 Mansfield, K. 2003. Marmoset models commonly used in biomedical research. *Comp. Med.* 53:383.
17 Sasaki, E., Suemizu, H., Shimada, A. et al. 2009. Generation of transgenic non-human primates with germline transmission. *Nature* 459:515.
18 Kohu, K., Yamabe, E., Matsuzawa, A. et al. 2008. Comparison of 30 immunity-related genes from the common marmoset with orthologues from human and mouse. *Tohoku J. Exp. Med.* 215:167.
19 Ito, M., Hiramatsu, H., Kobayashi, K. et al. 2002. NOD/SCID/gamma®(null) mouse: an excellent recipient mouse model for engraftment of human cells. *Blood* 100:3175.
20 Matsumura, T., Kametani, Y., Ando, K. et al. 2003. Functional CD5+ B cells develop predominantly in the spleen of NOD/SCID/gammac(null) (NOG) mice transplanted either with human umbilical cord blood, bone marrow, or mobilized peripheral blood CD34+ cells. *Exp. Hematol.* 34:1240.
21 Ito, M., Kobayashi, K. and Nakahata, T. 2008. NOD/Shi-scid IL2rgamma(null) (NOG) mice more appropriate for humanized mouse models. *Curr. Top. Microbiol. Immunol.* 324:53.
22 Kametani, Y., Shiina, M., Katano, I. et al. 2006. Development of human-human hybridoma from anti-Her-2 peptide-producing B cells in immunized NOG mouse. *Exp. Hematol.* 34:1240.
23 Ito, R., Shiina, M., Saito, Y., Tokuda, Y., Kametani, Y. and Habu, S. 2008. Antigen-specific antibody production of human B cells in NOG mice reconstituted with the human immune system. *Curr. Top. Microbiol. Immunol.* 324:95.
24 Kambe, N., Hiramatsu, H., Shimonaka, M. et al. 2004. Development of both human connective tissue-type and mucosal-type mast cells in mice from hematopoietic stem cells with identical distribution pattern to human body. *Blood* 103:860.
25 Kametani, Y., Suzuki, D., Kohu, K. et al. 2009. Development of monoclonal antibodies for analyzing immune and hematopoietic systems of common marmoset. *Exp. Hematol.* 37:1318.
26 Saito, H. 2006. Culture of human mast cells from hemopoietic progenitors. *Methods Mol. Biol.* 315:113.
27 Welker, P., Grabbe, J., Zuberbier, T., Guhl, S. and Henz, B. M. 2000. Mast cell and myeloid marker expression during early in vitro mast cell differentiation from human peripheral blood mononuclear cells. *J. Invest. Dermatol.* 114:44.
28 Izawa, K., Tani, K., Nakazaki, Y. et al. 2004. Hematopoietic activity of common marmoset CD34 cells isolated by a novel monoclonal antibody MA24. *Exp. Hematol.* 32:843.
29 Prasad, S., Kireta, S., Leedham, E., Russ, G. R. and Coates, P. T. 2010. Propagation and characterisation of dendritic cells from G-CSF mobilised peripheral blood monocytes and stem cells in common marmoset monkeys. *J. Immunol. Methods* 352:59.
30 Shizuru, J. A., Negrin, R. S. and Weissman, I. L. 2005. Hematopoietic stem and progenitor cells: clinical and preclinical regeneration of the hematolymphoid system. *Annu. Rev. Med.* 56:509.
31 Weissman, I. L. and Shizuru, J. A. 2008. The origins of the identification and isolation of hematopoietic stem cells, and their capability to induce donor-specific transplantation tolerance and treat autoimmune diseases. *Blood* 112:3543.
32 Gunji, Y., Nakamura, M., Osawa, H. et al. 1993. Human primitive hematopoietic progenitor cells are more enriched in KITlow cells than in KIThigh cells. *Blood* 82:3283.
33 Doulatov, S., Notta, F., Eppert, K., Nguyen, L. T., Ohashi, P. S. and Dick, J. E. 2010. Revised map of the human progenitor hierarchy shows the origin of macrophages and dendritic cells in early lymphoid development. *Nat. Immunol.* 11:585.
34 Geissmann, F., Manz, M. G., Jung, S., Sieweke, M. H., Merad, M. and Ley, K. 2010. Development of monocytes, macrophages, and dendritic cells. *Science* 327:656.
35 Hallgren, J. and Gurish, M. F. 2007. Pathways of murine mast cell development and trafficking: tracking the roots and routes of the mast cell. *Immunol. Rev.* 217:8.
36 Irani, A. M. and Schwartz, L. B. 1989. Mast cell heterogeneity. *Clin. Exp. Allergy* 19:143.

Oncolytic plasmid: A novel strategy for tumor immuno-gene therapy

CHIEKO YOSHIHARA[1], KATSUYUKI HAMADA[2], MINAKO KURODA[1] and YOSHIYUKI KOYAMA[1]

[1]Department of Textile Science, Otsuma Women's University, Tokyo 102-8357;
[2]Department of Obstetrics and Gynecology, School of Medicine, Ehime University, Ehime 791-0295, Japan

Received April 4, 2011; Accepted October 10, 2011

DOI: 10.3892/ol.2011.467

Abstract. The oncolytic virus is expected to proliferate in and destroy tumor cells. The virus is also thought to generate antitumor immunity. Virally infected tumor cells express viral antigens on their surfaces. Such tumor cells or their fragments would be taken up by antigen-presenting cells (APCs) together with tumor-associated antigens (TAAs), and facilitated cross-priming of tumor-specific T cells. Virus-specific protein presented on the infected cells therefore played a crucial role in the enhancement of the adaptive antitumor immunity. In this study, a plasmid encoding adenovirus protein, the adenovirus death protein (ADP), was constructed, and a very fine complex of the plasmid with polyethylenimine (PEI) and chondroitin sulfate (CS) was injected into tumor-bearing mice. Transfection of the ADP gene was shown to suppress tumor growth as effectively as granulocyte-macrophage colony-stimulating factor (GM-CSF) transfection. When mice were administered plasmid coding ADP (pDNA-ADP) to generate an immune response to ADP prior to therapy, transfection of the ADP gene induced a much higher level of tumor growth suppression than that found in the non-immunized mice. An evident synergistic effect of ADP and GM-CSF genes was also observed, and at a pDNA-ADP/pDNA-GM-CSF ratio of 4:1, significant suppression of tumor growth was achieved even in the non-immunized mice.

Introduction

Since oncolytic activity attributed to replicating viruses was previously reported by De Pace (1), a number of clinical trials were conducted using viruses to treat tumors. In the 1950s, virotherapy of cancer was started with the naturally occurring oncolytic virus, a virus capable of replicating specifically in tumor cells and causing specific lysis of cancer cells but not normal cells. Advancements in virotherapy were made following the development of the genetically engineered, replication-selective oncolytic virus in 1991 (2). Such oncolytic viruses are expected to proliferate in and destroy tumor cells.

However, preclinical and clinical data suggest that in some cases virotherapy may in fact act as cancer immunotherapy. Tumor-bearing mice injected with an oncolytic virus exhibited an antitumor immune response, and local injection of the oncolytic virus often caused regression of remote as well as peripheral tumors. It should be mediated by the systemic antitumor immune response. Tumor-specific cytotoxic T lymphocytes (CTL) activity against tumor cells persisted for a long period of time, and protection against tumor rechallenge was observed (3).

Viruses are thought to generate antitumor immunity. Virally infected tumor cells would express viral antigens on their surfaces, and effectively stimulate antigen-presenting cells (APCs) to cross-prime tumor-specific T cells (4). Virus-specific proteins presented on the infected tumor cells or their fragments thus appeared to play a crucial role in the enhancement of the adaptive antitumor immunity.

We thought that adaptive antitumor immunity might be induced not only by virus infection, but also by transfection of the gene encoding viral protein into the tumor cells. Extra viral genes would produce a viral antigen in the tumor cells, and cause the stimulation of APCs as well as viral-infected cells.

The question arises as to which of the virus proteins would be most effective in inducing antitumor immunity. Oncolytic adenoviruses have usually been engineered by deletion of E1 genes that are necessary for a virus to replicate in normal cells. E3 genes were often deleted to provide more space for therapeutic gene insertion. However, E3-positive (E3+) viruses were reported to kill tumor cells 1.6-20 times more effectively in different cell lines (5). Among the E3 proteins, the adenovirus death protein (ADP) has unique properties. ADP is an adenovirus nuclear membrane glycoprotein (6), and, unlike other E3 genes, ADP is expressed at late stages of infection. Whereas almost all other E3 genes have immunomodulatory functions, ADP is responsible for the efficient lysis and release of the progeny virus from the infected cell (7-9). Adenovirus, which overexpresses ADP, was also prepared by deleting the

Correspondence to: Dr Yoshiyuki Koyama, Department of Textile Science, Otsuma Women's University, Sanbancho, Chiyoda-ku, Tokyo 102-8357, Japan
E-mail: koyama@otsuma.ac.jp

Key words: gene therapy, adenovirus death protein, immunotherapy, plasmid, tumor

E3 region and reinserting the ADP gene, and was found to spread more rapidly and effectively through tumors, showing highly improved tumor growth regression (10).

In this study, plasmid DNA encoding ADP gene was constructed, and an extremely fine complex of the plasmid with polyethylenimine (PEI) and chondroitin sulfate (CS) was prepared by a previously reported method (11). The complex was injected into tumor-bearing mice, and the tumor growth inhibition effect was examined.

Materials and methods

Materials and animals. CS from shark cartilage was supplied by Seikagaku Corporation (Tokyo, Japan). Linear PEI 'MAX' (MW 40,000) was purchased from Polyscience, Inc. (Warrington, PA, USA).

Plasmid coding adenovirus ADP (pDNA-ADP) was constructed with the product of PCR conducted with ADP-S ATGACCAACACAACCAACGC and ADP-AS-1 ACTCGAGGAATCATGTCTCA as primers, the genome of adenovirus type 5 (Microbix Biosystems, Ontario, Canada) as a template, and Takara Ex Taq (Takara, Japan) as the enzyme. pDNA-ADP was first subcloned into pTAC-1, and its sequence was analyzed by ABI Sequencing Analysis. Finally, pDNA-ADP was inserted into pcDNA3.1(-) (Invitrogen, USA) with *Eco*RI and *Bam*HI, and the sequence was confirmed again by ABI Sequencing Analysis. Plasmid coding mouse granulocyte macrophage-colony stimulating factor (pDNA-GM-CSF) was similarly produced with pcDNA3.1 vector as previously reported (11). The plasmids were amplified, and purified by Mitsuwa Frontech Corp., Japan.

Cytotoxic activity of the ADP plasmid complex

Preparation of DNA complex. CS solution (267 μg in 600 μl) and PEI solution (132 μg in 300 μl), respectively, were added in this order to a solution of plasmid DNA coding ADP or luciferase (45 μg in 300 μl). The solutions were previously prepared in 7 mM phosphate buffer (PB). After 30 min, the mixture was diluted by condensed PBS to afford an isotonic solution containing a given amount of the plasmid complex.

Evaluation of the cytotoxicity. B16 cells, a mouse melanoma cell line, were seeded onto 96-well plates at 7.5×10^4 cells per well, and cultured for 2 days in Gibco minimum essential medium (MEM) supplemented with 10% fetal bovine serum (FBS), penicillin G sodium (100 U/ml), and streptomycin sulfate (0.1 mg/ml). The primary growth medium was then replaced with 100 μl of fresh MEM with FBS and antibiotics. Fresh or lyophilized-and-rehydrated plasmid DNA complex suspensions prepared above were added to the cells (100 μl/well), and incubated for 4 h at 37°C. Fresh medium was added to the wells (100 μl/well), and after an additional incubation at 37°C (20 or 68 h), cell viability was measured by WST-1 assay.

Therapeutic effect of the ADP plasmid complex

Preparation of freeze-dried DNA complex. CS solution (594 μg in 118.7 μl) and PEI solution (294 μg in 58.8 μl), respectively, were added in this order to a plasmid DNA coding ADP or mouse GM-CSF solution (100 μg in 4.82 ml). All the solutions were previously prepared in 7 mM PB. After standing for 20 min, the complex of plasmid-ADP and that made of plasmid-GM-CSF was mixed at the given ratio. Dextran solution in H_2O (10%, 50 μl) was added, and the mixture was freeze-dried, and stored at 4°C. It was rehydrated with 250 μl of H_2O just before use.

Immunization. Immunization was performed by intramuscular injection of pDNA-ADP (10 μg in 50 μl PBS) into the left posterior leg of male ddY mice 3 weeks prior to inoculation of B16 cells.

Therapeutic effect on the tumor-bearing mice. Male C57BL/6 mice (5 weeks) were inoculated subcutaneously with $2.0\text{-}2.7 \times 10^6$ B16 cells. When the size of the tumor reached 3-4 mm in diameter, the animals were intratumorally injected with the rehydrated plasmid complex (containing 100 μg of plasmid) five times every other day. The tumor diameter was measured every day for 25 days, and the tumor size was calculated as $(4/3)\pi ab^2$, where a is the long axis and b the short axis of the solid tumor. The care and use of laboratory animals followed the guidelines for animal experiments of the institutes involved.

Results

Preparation of the small DNA complex particle suspension. Extremely small DNA complex particles were obtained by mixing the plasmid/CS premixed solution with PEI at a very low concentration, followed by the lyophilyzed-and-rehydrated condensation procedure, as previously reported (11). Particle size analysis using a laser-diffraction particle size analyzer showed that 50% of the complexes were no more than 150 nm in diameter.

Cytotoxic activity of the pDNA-ADP complex. The cultured B16 melanoma cells were treated with the pDNA-ADP complex, and the survival percentage compared to the non-treated control was estimated by WST-1 assay. The survival rate in the cells treated with pDNA-luciferase complex was also simultaneously examined. As shown in Fig. 1, after 24 h incubation with 10 μg/ml of pDNA-ADP complex, cell survival was almost 60%, as was the case with the pDNA-luciferase complex. After 72 h treatment with the pDNA-ADP complex, a reduction of approximately 50% was observed, while the cells transfected with the luciferase gene still showed a relatively high rate (75%).

Therapeutic effect of the pDNA-ADP complex on tumor-bearing mice. Small DNA/PEI/CS complex was prepared with pDNA-ADP, and intratumorally injected five times every other day into immunized or non-immunized male C57BL/6 mice bearing subcutaneous B16 tumors. The results of the pDNA-ADP complex and the pDNA-GM-CS complex are shown in Fig. 2. Rapid growth of the tumor was observed in all the control non-treated mice. In the non-immunized mice, the pDNA-ADP complex showed as effective a suppression of tumor growth as the pDNA-GM-CSF complex, which exhibited a high therapeutic effect, as shown in our previous study (11). When mice were administered pDNA-ADP prior to therapy to generate an immune response to ADP, transfection of the ADP gene induced a much higher level of tumor growth suppression than in the non-immunized mice, whereas

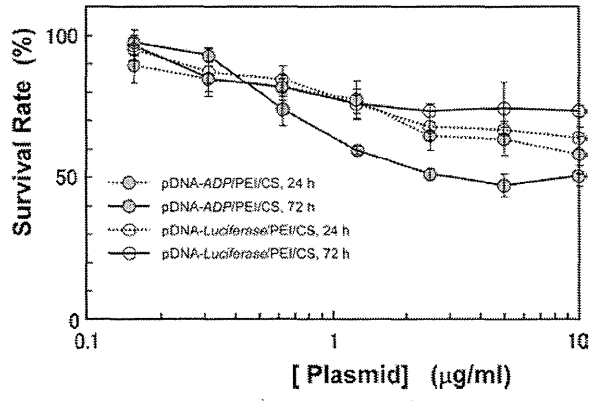

Figure 1. Cytotoxicity of plasmid complexes. Each complex was incubated with B16 melanoma cells for 24 or 72 h at the given concentrations.

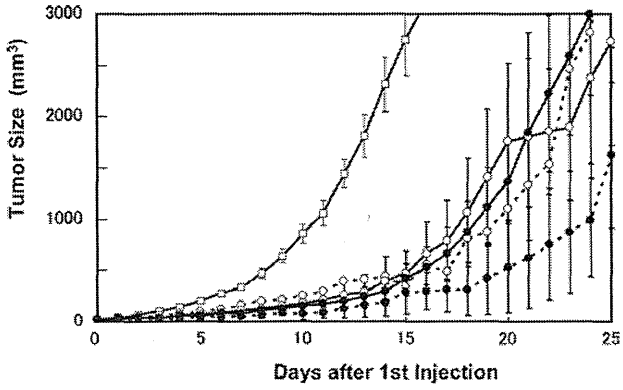

Figure 2. *In vivo* effects of tumor treatment with pDNA-ADP complex (closed circle), or pDNA-GM-CSF complex (open circle), on the non-immunized mice (solid line) or the mice pre-immunized by intramuscular injection of pDNA-ADP (dotted line). The open square expresses the results with control non-treated mice. Each complex containing 100 μg of the plasmid was intratumorally injected five times every other day into male C57BL/6 mice bearing subcutaneous B16 melanoma solid tumors. Tumor volume was expressed as the mean ± SE (n=5).

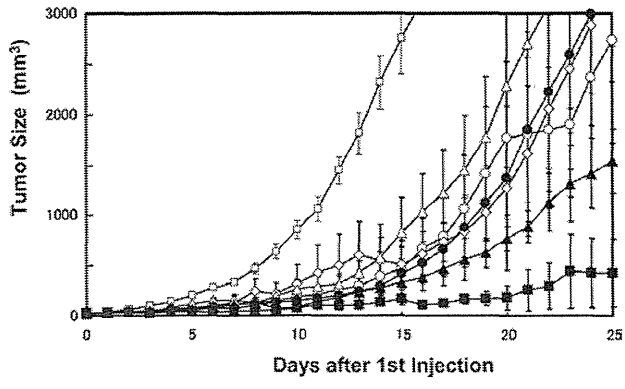

Figure 3. *In vivo* effects of tumor treatment with the complexes comprising pDNA-ADP+pDNA-GM-CSF at ratios of 0:5 (open circle), 1:4 (open diamond), 2:3 (open triangle), 3:2 (closed triangle), 4:1 (closed square), and 5:0 (closed circle) on the non-immunized mice. The open square expresses the results with control non-treated mice. Each complex containing 100 μg of the plasmid was intratumorally injected five times every other day into male C57BL/6 mice bearing subcutaneous B16 melanoma solid tumors. Tumor volume was expressed as the mean ± SE (n=5).

the therapeutic effect by the GM-CSF gene was no different between the immunized and non-immunized groups.

The effect of the simultaneous co-transfection of pDNA-ADP and pDNA-GM-CSF (total 100 μg of the plasmid per mouse) was examined at various pDNA-ADP/pDNA-GM-CSF ratios on the non-immunized mice. As shown in Fig. 3, an evident synergistic effect of the genes was observed, and significant suppression of tumor growth was observed even in the non-immunized mice. The highest therapeutic effect was obtained at plasmid-ADP/plasmid-GM-CSF at a ratio of 4:1, and the tumor volume was maintained <5 times as large as at the beginning of treatment for 20 days, while that in the control mice became 10 times larger in 10 days.

Discussion

Cytotoxic activity of the pDNA-ADP complex. ADP has been reported to be associated with a cell lytic activity of adenovirus. Transfection of the ADP gene to cultured cells was therefore expected to show cytotoxic activity. Induction of cytotoxicity by ADP-transfection was higher than that by pDNA-luciferase, but not as high as expected from the cell lytic activity reported. The duration of the plasmid-gene expression, or the protein production may not be sufficient to express strong cell lytic phenomena. Otherwise, ADP may not be capable of cell killing activity by itself. Another adenovirus death factor, E4orf4, was also found to induce cell death and suggested to collaborate with ADP in the induction of cell lysis and progeny release (12).

Therapeutic effect of the pDNA-ADP complex on tumor-bearing mice. In the non-immunized mice, the pDNA-ADP complex was found to be as effective in the suppression of tumor growth as GM-CSF. The effect of the ADP transfection was strongly enhanced by pre-immunization of mice with ADP-coding plasmid. Pre-existing anti-ADP antibody or ADP-specific CTL in the immunized mice would be attributed to the rapid response in the early therapeutic stage.

In *in vivo* therapy for tumors, GM-CSF is often used as an immunomodulatory agent. Oncolytic viruses engineered to secrete GM-CSF have been reported to show higher antitumor activity (13). Co-injection of GM-CSF-expressing virus also enhanced the anticancer effect of oncolytic viruses (14). The simultaneous co-transfection of the ADP and GM-CSF genes was subsequently attempted to examine the synergistic effect of the proteins on tumor growth suppression. As expected, a much higher therapeutic effect was obtained even in the non-immunized mice at a plasmid-ADP/plasmid-GM-CSF ratio of 3:2 and 4:1. GM-CSF is known to recruit and stimulate DCs in viral tumor therapy (15). The activity of DCs against ADP-expressing tumor cells would be enhanced by the cytokines.

In our previous study, an allogeneic model, B16 melanoma cells in ddY mice, was used allowing pDNA-GM-CSF to exhibit complete regression of the tumor (11). In the present study, a syngeneic model was employed in which tumor growth is more rapid than in the allogeneic model, and the effect of the transfection of the GM-CSF gene was not so strong as to completely inhibit the tumor growth. In the syngeneic model, tumor cells may escape from immune surveillance since the

cells are altered cells derived from genetically identical mice. GM-CSF expression may not be enough to prevent tumor escape in a syngeneic model.

Tumor escape from the immune system is most often caused by weak immunogenicity of tumor-associated antigens (TAAs), and has been a major problem in immunotherapy. Various DNA vaccine encoding TAAs have been developed and applied in antitumor immunotherapy. However, the activation of immunity against poorly immunogenic tumor antigens is difficult. Weber *et al* reported that vaccination of mice with DNA encoding cancer differentiation antigens is ineffective when self-DNA is used (16). These authors showed a high potential of the orthologous DNA from another species. To conquer the disadvantage of weak immunogenicity, Bergman *et al* developed the xenogeneic DNA vaccination (17). Injection of the plasmid encoding human tyrosinase into dogs bearing melanoma was capable of breaking tolerance against a self-tumor differentiation antigen, leading to high clinical responses.

In this study, a viral protein, ADP, was transfected on the tumor cells. ADP is an integral membrane glycoprotein that localizes to the inner and outer nuclear membrane and the Goldi apparatus. Some ADP molecules may also exist on the cell surface membrane, or at least appear on the apoptotic tumor cell fragments. These fragments would be captured by and stimulate APCs to mature and cross-prime T cells against both ADP and TAAs.

Since Tang *et al* demonstrated that plasmid DNA induces the formation of antibodies against an encoded protein (18), there has been rapid progress in the DNA vaccine, and it has now been accepted as a promising therapy for tumors. Prior identification of each tumor-related antigen is required for peptide-based immunotherapy. The transfection of ADP is apparently effective in various types of tumor. The elicitation of immune response towards tumor antigens by the transfection of such viral protein genes into tumor cells is likely to be a breakthrough in genetic immunotherapy.

References

1. De Pace NG: Sulla scomparsa di un enorme cancro vegetante del collo dell'utero senza cura chirurgica. Ginecologia 9: 82-88, 1912.
2. Martuza RL, Malick A, Markert JM, Ruffner KL and Coen DM: Experimental therapy of human glioma by means of a mutant. Science 252: 854-856, 1991.
3. Todo T, Rabkin SD, Sundaresan P, Wu A, Meehan KR, Herscowitz HB and Martuza RL: Systemic antitumor immunity in experimental brain tumor therapy using a multimutated, replication-competent herpes simplex virus. Hum Gene Ther 10: 2741-2755, 1999.
4. Prestwich RJ, Harrington KJ, Pandha HS, Vile RG, Melcher AA and Errington F: Oncolytic viruses: a novel form of immunotherapy. Expert Rev Anticancer Ther 8: 1581-1588, 2008.
5. Suzuki K, Alemany R, Yamamoto M and Curiel DT: The presence of the adenovirus E3 region improves the oncolytic potency of conditionally replicative adenoviruses. Clin Cancer Res 8: 3348-3359, 2002.
6. Wold WSM, Cladaras C, Magie SC and Yacoub N: Mapping a new gene that encodes an 11,600-molecular-weight protein in the E3 transcription unit of adenovirus 2. J Virol 52: 307-313, 1984.
7. Tollefson AE, Ryerse JS, Scaria A, Hermiston TW and Wold WS: The E3-11.6-kDa adenovirus death protein (ADP) is required for efficient cell death: characterization of cells infected with adp mutants. Virology 220: 152-162, 1996.
8. Wold WSM, Doronin K, Toth K, Kuppuswamy M, Lichtenstein DL and Tollefson AE: Immune responses to adenoviruses: viral evasion mechanisms and their implications for the clinic. Curr Opin Immunol 11: 380-386, 1999.
9. Tollefson AE, Scaria A, Hermiston TW, Ryerse JS, Wold LJ and Wold WS: The adenovirus death protein (E3-11.6K) is required at very late stages of infection for efficient cell lysis and release of adenovirus from infected cells. J Virol 70: 2296-2306, 1996.
10. Doronin K, Toth K, Kuppuswamy M, Ward P, Tollefson AE and Wold WS: Tumor-specific, replication-competent adenovirus vectors overexpressing the adenovirus death protein. J Virol 74: 6147-6155, 2000.
11. Ito T, Yoshihara C, Hamada K and Koyama Y: DNA/polyethyl eneimine/hyaluronic acid small complex particles and tumor suppression in mice. Biomaterials 31: 2912-2918, 2010.
12. Lavoie JN, Nguyen M, Marcellus RC, Branton PE and Shore GC: E4orf4, a novel adenovirus death factor that induces p53- independent apoptosis by a pathway that is not inhibited by zVADfmk. J Cell Biol 140: 637-645, 1998.
13. Malhotra S, Kim T, Zager J, Bennett J, Ebright M, D'Angelica M and Fong Y: Use of an oncolytic virus secreting GM-CSF as combined oncolytic and immunotherapy for treatment of colorectal and hepatic adenocarcinomas. Surgery 141: 520-529, 2007.
14. Hamada K, Desaki J, Nakagawa K, Zhang T, Shirakawa T, Gotoh A and Tagawa M: Carrier cell-mediated delivery of a replication-competent adenovirus for cancer gene therapy. Mol Ther 15: 1121-1128, 2007.
15. Todo T, Rabkin SD, Sundaresan P, Wu A, Meehan KR, Herscowitz HB and Martuza RL: Systemic antitumor immunity in experimental brain tumor therapy using a multimutated, replication-competent herpes simplex virus. Hum Gene Ther 10: 2741-2755, 1999.
16. Weber LW, Bowne WB, Wolchok JD, Srinivasan R, Qin J, Moroi Y, Clynes R, Song P, Lewis JJ and Houghton AN: Tumor immunity and autoimmunity induced by immunization with homologous DNA. J Clin Investig 102: 1258-1264, 1998.
17. Bergman PJ, McKnight J, Novosad A, Charney S, Farrelly J, Craft D, Wulderk M, Jeffers Y, Sadelain M, Hohenhaus AE, Segal N, Gregor P, Engelhorn M, Riviere I, Houghton AN and Wolchok JD: Clin Cancer Res 9: 1284-1290, 2003.
18. Tang DC, DeVit M and Johnston SA: Genetic immunization is a simple method for eliciting an immune response. Nature 356: 152-154, 1992.

Improved Gene Transfer into Bladder Cancer Cells Using Adenovirus Vector Containing RGD Motif

KAZUHIRO HIWASA[1], HISAO NAGAYA[1], SHUJI TERAO[1], BISHNU ACHARYA[1], KATSUYUKI HAMADA[2], HIROYUKI MIZUGUCHI[3] and AKINOBU GOTOH[1]

[1]*Laboratory of Cell and Gene Therapy, Institute for Advanced Medical Sciences, Hyogo College of Medicine, Nishinomiya, Japan;*
[2]*Department of Obstetrics and Gynecology, Ehime University School of Medicine, Matsuyama, Japan;*
[3]*Laboratory of Biochemistry and Molecular Biology, Graduate School of Pharmaceutical Sciences, Osaka University, Suita, Japan*

Abstract. *Background: The transduction efficacy of adenovirus serotype 5 (Ad5) vector in high-grade human bladder cancer cells is generally extremely low due to the non-expression of coxsackie and adenoviral receptor (CAR). We investigated whether fiber-modified adenovirus vector containing an RGD motif in the HI loop of the adenovirus fiber knob could increase the transduction efficiency of Ad5 into human bladder cancer cells in vitro. Materials and Methods: We examined the expressions of CAR, and of α_v, β_3 and β_5 integrin, and the transduction efficacy of fiber-modified adenovirus vector in four human bladder cancer cell lines (TCC-SUP, 253J, T24 and KK47). Results: The expression of CAR was lower and those of α_v and β_3 integrin were higher in four human cancer cell lines compared with the control cell line, KK47. The transduction efficacy of fiber-modified adenovirus vector increased by 20- to 470-fold compared with Ad5. Conclusion: Fiber-modified adenovirus vector may be useful in order to establish new effective gene therapy strategies for the treatment of high-grade human bladder cancer.*

Adenoviruses are useful vectors for cancer gene delivery because of the high gene transfer efficacy, high titer production, and safety (1, 2). Recombinant adenovirus 5 (Ad5) has been widely used in gene transfer experiments and clinical gene therapy. Entry of Ad5 into the host cell is initiated by the knob domain of the fiber protein binding to the cell receptor, coxsackie and adenoviral receptor (CAR) (3). This is followed by a secondary interaction, where an Arg-Gly-Asp (RGD) motif in the penton base interacts with an α_v-containing integrin, particularly $\alpha_v\beta_3$ and/or $\alpha_v\beta_5$ integrin. Binding to α_v integrin results in endocytosis of the virus particle *via* clathrin-coated pits (4). However, the loss or decrease of CAR expression has been observed in various types of cancer, including bladder cancer (5-7). In an effort to target bladder cancer one needs to either increase the expression of CAR or to increase the transduction efficacy of Ad5 vector using CAR-independent tropism. Mizuguchi and Hayakawa have developed vectors with improved tropism by altering the fiber protein (8).

Fiber-modified adenovirus vector containing an RGD motif in the HI loop of the fiber knob (Ad5RGD vector) is capable of CAR-independent tropism in target cell expressing $\alpha_v\beta_3$ or $\alpha_v\beta_5$ integrin on the membrane (9). We showed that the Ad5RGD vector is capable of inducing much higher transduction efficacy for human renal cell carcinoma cells than the Ad5 vector (10)

In the present study, we examined the transduction efficacy of the Ad5 and Ad5RGD vectors in several human bladder cancer cell lines.

Materials and Methods

Cell lines and cell culture. Established cell lines derived from human bladder carcinoma cell lines, namely, TCC-SUP, 253J and T24, were obtained from the American Type Culture Collection (Manassas, VA, USA); the KK47 human bladder cancer cell line was generously provided by Dr. Seiji Naito (Department of Urology, Kyushu University, Fukuoka, Japan). In the present study, we maintained TCC-SUP, 253J, T24 and KK47 cells in Roswell Park Memorial Institute-1640 medium (Life Technologies, Inc., Gaithersburg, MD, USA), containing 10% fetal bovine serum and antibiotics (50 μg/ml streptomycin sulfate and 50 IU/ml of penicillin). All cell lines were maintained at 37°C in a humidified

Correspondence to: Akinobu Gotoh, M.D., Ph.D., Professor of the Laboratory of Cell and Gene Therapy Institute for Advanced Medical Sciences, Hyogo College of Medicine, 1-1 Mukogawa-cho, Nishinomiya 663-8501, Japan. Tel: +81 798456807, Fax: +81 798456806, e-mail: gotoh@hyo-med.ac.jp

Key Words: Adenovirus vector, transduction efficacy, RGD, bladder cancer cell lines.

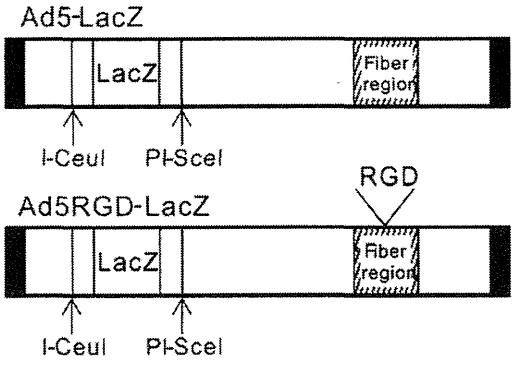

Figure 1. *Schematic representation of adenovirus. LacZ, β-galactosidase under CMV promoter; RGD, Arg-Gly-Asp motif; I-CeuI, I-CeuI restriction enzyme recognition sequence; PI-SceI, PI-SceI restriction enzyme recognition sequences.*

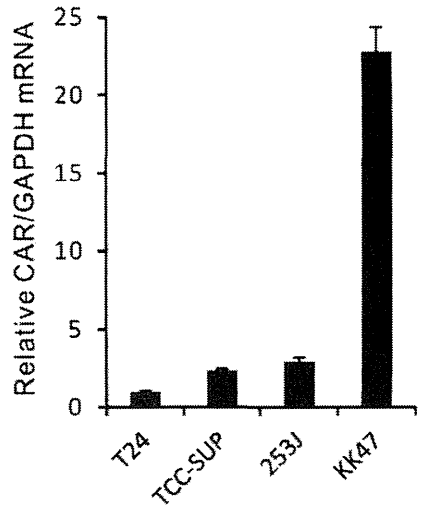

Figure 2. *Relative mRNA levels of coxsackie and adenoviral receptor (CAR) by quantitative reverse transcription-PCR in human bladder cancer cell lines. The relative expression level of T24 was set to 1. Glyceraldehyde-3-phosphate dehydrogenase (GAPDH) was selected as an endogenous RNA control to normalize for differences in the amount of total RNA. Values are means±SD (n=3).*

Table I. *Primer sequences used for PCR amplification.*

Gene		Sequence
CAR	Forward	5'-CAGAAGCTACATCGGCAGTAATCA-3'
	Reverse	5'-CTCTGAGGAGTGCGTTCAAAGTC-3'
	Probe	5'-d FAM-TCCATGTCTCCTTCCAACATGGAAGGA-TAMRA-3'
α_v Integrin	Forward	5'-CAACGTGAGCGGGACCAT-3'
	Reverse	5'-TTGGCAGACAATCTTCAAGCA-3'
	Probe	5'-d FAM-TCATCACTAAGCGGGATCTTGCCCTCA-BHQ-1- 3'
β_3 Integrin	Forward	5'-CCCTCGAAAACCCCTGCTAT-3'
	Reverse	5'-TTAGCGTCAGCACGTGTTTGTAG-3'
	Probe	5'-d FAM-TATGAAGACCACCTGCTTGCCCATGTTT-BHQ-1-3'
β_5 Integrin	Forward	5'-GGCTGGGACGTCATTCAGAT-3'
	Reverse	5'-AGCTGGAAGGTGGTCTTGTCA-3'
	Probe	5'-d FAM-ACACCACAGGAGATTGCCGTGAACCT-BHQ-1-3'
GAPDH	Forward	5'-GAAGGTGAAGGTCGGAGTC-3'
	Reverse	5'-GAAGATGGTGATGGGATTTC-3'
	Probe	5'-d FAM-CAAGCTTCCCGTTCTCAGCC-BHQ-1-3'

CAR: coxsackie and adenoviral receptor, GAPDH: Glyceraldehyde -3-phosphate dehydrogenase.

incubator with an atmosphere of 5% CO_2 and 97% relative humidity, and were subcultured on reaching 80% confluence using trypsin-EDTA. The cells were transferred two or three times a week into fresh growth medium.

Adenovirus vector preparation. We examined the transduction efficacy of Ad5-LacZ, constructed as previously described (11), and of Ad5RGD-LacZ, containing an RGD peptide in the HI loop of the fiber knob (9, 10) (Figure 1). The viruses were purified by double cesium chloride gradient ultracentrifugation using standard methods. Serial dilutions of the viruses were used to infect HEK 293 cell (RIKEN Bioresource Center, Tsukuba, Japan) for a plaque assay. Titers of adenovirus vectors were assessed using the 50% tissue culture infectious dose method and were expressed as plaque-forming units (pfu)/ml (Ad5-LacZ, 3.6×10^{11} pfu/ml; Ad5RGD-LacZ, 1.1×10^{11} pfu/ml).

In vitro real-time quantitative reverse transcription-PCR assay. Total cellular RNA was isolated from all cell lines using a TaKaRa RNA extraction KIT (Takara Bio Inc., Shiga, Japan), and was reverse transcribed using a reverse transcription kit (TaKaRa RNA PCR Kit Ver. 3.0), following the manufacturer's protocol. The resulting cDNA was amplified with CAR, α_v integrin, β_3 integrin, β_5 integrin, and glyceraldehyde -3-phosphate dehydrogenase (GAPDH) sequence-specific primers (40 cycles: 95°C for 15 s, 60°C for 1 min) using TaqMan chemistry in the StepOnePlus Real-Time PCR System v2.0 (Applied Biosystems Japan Ltd., Tokyo, Japan). Table I shows the sequences of the TaqMan probes and primers for CAR, α_v integrin, β_3 integrin, β_5 integrin, and GAPDH. All primers and probes were purchased from Biosearch Technologies Japan (Tokyo, Japan).

Transduction efficacy of adenovirus vectors. In order to determine the transduction efficacy in each cell line, 2.5×10^4 cells were prepared in a 24-well plate and infected with Ad5-LacZ or Ad5RGD-LacZ. After 48 h, the transduction efficacy was assessed by β-galactosidase (β-gal) staining and expressed as blue titer units (btu)/ml.

Statistical analysis. Statistical significance was determined by using analysis of variance (ANOVA) and Bonferroni correction, with $p<0.01$ considered to be statistically significant.

Results

Relative quantification of mRNA expression of CAR. The mean relative quantification of *CAR* mRNA expression detected in the cell lines used in this study, is shown in Figure 2. In order to normalize for differences in the amount of total RNA, GAPDH was used as an endogenous RNA control. The relative quantification was calculated by

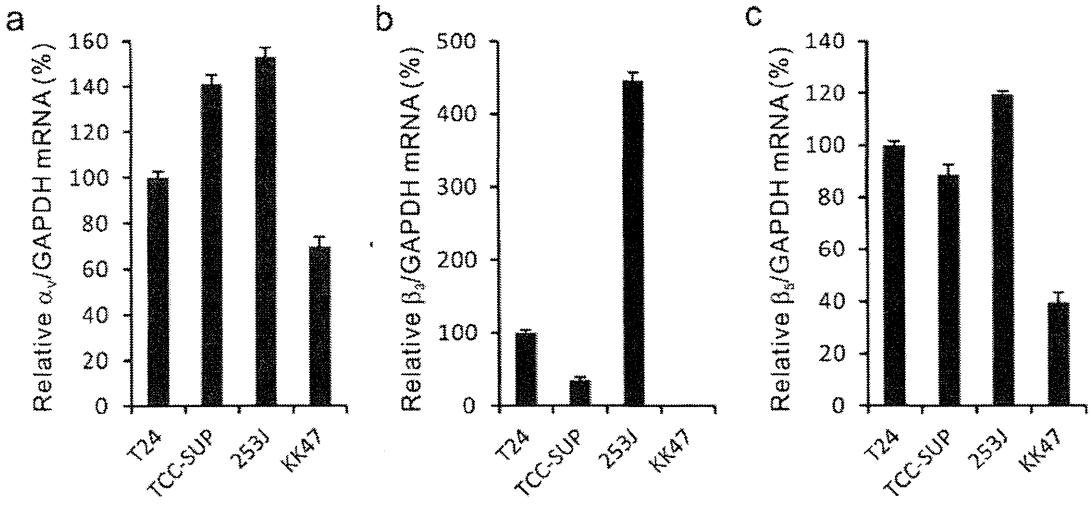

Figure 3. *Relative mRNA levels of α_v integrin (a), β_3 integrin (b) and β_5 integrin (c) obtained by quantitative reverse transcription-PCR in human bladder cancer cell lines. The relative expression level of T24 was set to 100. Glyceraldehyde-3-phosphate dehydrogenase (GAPDH) was selected as an endogenous RNA control to normalize for differences in the amount of total RNA. Values are means±SD (n=3).*

dividing by the value of RNA obtained for T24 cells. The levels of *CAR* mRNA expression were considerably higher in KK47 cells compared with the other cell lines.

Relative quantification of mRNA expressions of α_v, β_3 and β_5 integrins. The mean relative quantifications of *α_v integrin*, *β_3 integrin* and *β_5 integrin* mRNA expression detected in the cell lines used in this study are shown in Figure 3. The relative quantification was calculated by dividing by the value obtained for T24 cells. *α_v* and *β_5 integrin* mRNA were found to be uniformly expressed among the four cell lines. *β_3 Integrin* mRNA expression in 253J cells was found to be approximately four-fold higher than that of T24 and TCC-SUP cells. On the other hand KK47 was found to have minimal expression of *β_3 integrin* mRNA.

Transduction efficacy of adenovirus vectors. In order to assess the transduction efficacy in all cell lines, cells were infected with both Ad5-LacZ and Ad5RGD-LacZ. The transduction efficacy for each cell line was significantly increased by 470-, 20-, and 23-fold in T24, TCC-SUP, and 253J cells, respectively, using the RGD-bearing adenovirus, compared with the Ad5-LacZ ($p<0.01$) (Figure 4).

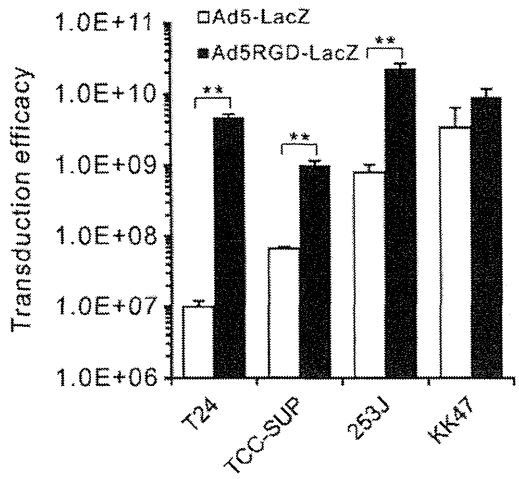

Figure 4. *The transduction efficacy of Ad5-LacZ and Ad5RGD-LacZ in human bladder cancer cell lines. Values are means±SD (n=3). Double asterisks indicate a significant increase compared to the transduction efficacy of Ad5-LacZ ($p<0.01$).*

Discussion

Ad5 vectors are one of the most studied vectors for gene therapy, as safety data for Ad5 have been excellent. However, the main disadvantage of the current therapies is that low transduction efficacy of Ad5 vectors limits the efficacy of treatment. Thus for successful cancer gene therapy, transduction efficacy of Ad5 vectors needs to be improved. In the present study, we attempted to increase the transduction efficacy of adenovirus vectors in bladder cancer cells.

Our present results revealed that the transduction efficiency in each of the bladder cancer cell lines tested, paralleled the relative quantification of *CAR* mRNA expression. To increase

transduction efficacy of adenovirus vectors, we tested the Ad5RGD vector. Indeed, our data revealed that the fiber-modified Ad5RGD vector achieved significantly higher transduction levels in all human bladder cancer cells as compared to the Ad5 vector itself. Oncolytic adenoviruses are being considered as a new therapeutic option for treatment of refractory disseminated cancer, including bladder cancer. Previously we demonstrated an antitumor effect in KK47 cells both *in vitro* and *in vivo* using an oncolytic Ad5 vector containing the *E1a* gene, controlled by the tumor-specific midkine promoter (12). However, the antitumor effect was considerably lower in T24 cells compared with KK47 cells *in vitro*. One reason for such a result for T24 cells is the low transduction efficiency of Ad5 vector into these cells because of their low CAR expression. Therefore, our results also suggest that if we can construct an oncolytic Ad5 virus containing the *E1a* gene controlled by midkine promoter, which has an inserted RGD motif, it may be possible to achieve a higher antitumor effect in bladder cancer cells with low CAR expression, including T24 cells, compared with gene therapy using a conventional Ad5 vector.

In this study, we demonstrated a dramatic increase in transduction efficacy in bladder cancer cells using an adenovirus vector containing the RGD motif on the HI loop of the fiber knob. Therefore, it may be preferable to use the fiber-modified adenovirus vector described in this study to target bladder cancer cells, and by applying our findings, it may be possible to establish new effective gene therapy strategies for the treatment of bladder cancer.

Acknowledgements

This study was supported by Grant-in-Aid for Scientific Research from the Japan Society for the Promotion of Science. The Authors wish to thank Satoko Kodama for her help in the completion of the manuscript.

References

1 Guse K, Cerullo V and Hemminki A: Oncolytic vaccinia virusfor the treatment of cancer. Expert Opin Biol Ther *11*: 595-608, 2011.

2 Bauerschmitz GJ, Barker SD and Hemminki A: Adenoviral genetherapy for cancer: from vectors to targeted and replication competentagents (review). Int J Oncol *21*: 1161-1174, 2002.

3 Bergelson JM, Cunningham JA, Dorguett G, Kurt-Jones EA, Krithivas A, Hong JS, Horwitz MS, Crowel RL and Finberg RW: Isolation of a common receptor for Coxsackie B viruses and adenovirus 2 and 5. Science *275*: 1320-1323, 1997.

4 Wickham TJ, Mathias P, Cheresh DA and Nemerow GR: Integrins alpha v beta 3 and alpha v beta 5 promote adenovirus internalization but not virus attachment. Cell *73*: 309-319, 1993.

5 Li Y, Pong RC, Bergelson JM, Hall MC, Sagalowsky AI, Tseng CP, Wang Z and Hsieh JT: Loss of adenoviral receptor expression in human bladder cancer cells: a potential impact on the efficacy of gene therapy. Cancer Res *59*: 325-330, 1999.

6 Okegawa T, Pong RC, Bergelson JM, Segalowsky AI and Hseieh JT: The mechanism of growth inhibitory effect of coxsackie and adenovirus receptor (CAR) on human bladder cancer: a functional analysis of CAR protein structure. Cancer Res *61*: 6592-6600, 2001.

7 Sachs, MD, Rauen KA, Ramamurthy M, Dodson JL, De marzo AM, Putzi MJ, Schoenberg MP and Rodriguez R: Integrin alpha v and coxsackie adenovirus receptor expression in clinical bladder cancer. Urology *60*: 531-536, 2002.

8 Mizuguchi H and Hayakawa T: Targeted adenovirus vectors. Hum Gene Ther *15*: 1034-1044, 2004.

9 Koizumi N, Mizuguchi H, Kondon M, Fuji M, Nakanishi T, Utoguchi N and Watanabe Y: Efficient gene transfer into differentiated human trophoblast cells with adenovirus vector containing RGD motif in the fiber protein. Biol Pharm Bull *29*: 1297-1299, 2006.

10 Terao S, Achaya B, Suzuku T, Naoe M, Hamada K, Mizuguchi H and Gotoh A: Improved gene transfer into renal carcinoma cells using adenovirus vector containing RGD motif. Anticancer Res *29*: 2997-3001, 2009.

11 Cruel DT: The development of conditionally replicative adenovirus for cancer therapy. Clin Canao Scer Res *6*: 3395-3399, 2000.

12 Terao S, Shirakawa T, Kobo S, Bishnu A, Lee SJ, Goda K, Tsukuda M, Hamada K, Tagawa M, Takenaka A, Fujisawa M and Gotoh A: Midkine promoter-based conditionally replicative adenovirus for targeting midkine-expressing human bladder cancer model. Urology *70*: 1009-1013, 2007.

Received March 30, 2012
Revised May 14, 2012
Accepted May 15, 2012

THE JOURNAL OF GENE MEDICINE
J Gene Med 2012; 14: 120–127.
Published online in Wiley Online Library (wileyonlinelibrary.com) **DOI:** 10.1002/jgm.1647

RESEARCH ARTICLE

Antitumor effect of chondroitin sulfate-coated ternary granulocyte macrophage-colony-stimulating factor plasmid complex for ovarian cancer

Katsuyuki Hamada[1]*
Chieko Yoshihara[2]
Tomoko Ito[3]
Kenzaburo Tani[4]
Masatoshi Tagawa[5]
Norio Sakuragawa[6]
Hiroshi Itoh[7]
Yoshiyuki Koyama[2]

[1]*Department of Obstetrics and Gynecology, School of Medicine, Ehime University, Shitsukawa, Toon, Ehime, Japan*

[2]*Department of Textile Science, Otsuma Women's University, Sanbancho, Chiyoda-ku, Tokyo, Japan*

[3]*Research Institute of Pharmaceutical Sciences, Musashino University, Shinmachi, NishiTokyo-shi, Tokyo, Japan*

[4]*Department of Advanced Molecular and Cell Therapy, Kyushu University Hospital, Kyushu University, Maidashi, Higashi-ku, Fukuoka, Japan*

[5]*Division of Pathology and Cell Therapy, Chiba Cancer Center Research Institute, Nitona, Chuo-ku, Chiba, Japan*

[6]*Bioresource Application Institute, Gamagori, Aichi, Japan*

[7]*Animal Medical Center, Tokyo University of Agriculture and Technology, Saiwai-cho, Fuchu-shi, Tokyo, Japan*

*Correspondence to: K. Hamada, Department of Obstetrics and Gynecology, School of Medicine, Ehime University, Shitsukawa, Toon, Ehime 791–0295, Japan.
E-mail: hamakatu@m.ehime-u.ac.jp

Received: 15 June 2011
Revised: 23 November 2011
Accepted: 20 December 2011

Abstract

Background Although replication-competent viruses have been developed for treating cancers, their cytotoxic effects are insufficient as a result of infection inhibited by the generation of neutralizing antibodies, and systemic administration is difficult as a result of the life-threatening serious side-effects of virus-induced cytokine surge. To overcome these critical problems, we devised a plasmid/polycation/polyanion complex and assessed the potential of ternary plasmid complexes coated with chondroitin sulfate in gene therapy for ovarian cancer. The antitumor effects of chondroitin sulfate-coated complex as an anionic component were compared with those of hyaluronic acid on ovarian cancer.

Methods Plasmid harboring the gene of murine granulocyte macrophage-colony-stimulating factor (mGM-CSF) was complexed with polyethyleneimine (PEI) and hyaluronic acid or chondroitin sulfate. Murine ovarian cancer cells were injected into (C57BL/6 × C3H/He) F_1 mice to prepare a subcutaneous or intraperitoneal tumor model.

Results DNA/PEI was charged positively and DNA/PEI/chondroitin sulfate or DNA/PEI/hyaluronic acid was charged negatively. Plasmid-green fluorescent protein (GFP)/PEI coated with 10-kilodalton (kDa) chondroitin sulfate increased transfection efficiency compared to coating with chondroitin sulfate of higher-molecular-weight or hyaluronic acid. The transfection efficiency of GFP/PEI/10-kDa chondroitin sulfate in ovarian cancer cells was six-fold higher than that in normal cells. Intraperitoneal injection of mGM-CSF/PEI coated with 10-kDa chondroitin sulfate prolonged survival compared to that coated with hyaluronic acid. Intratumoral injection of mGM-CSF/PEI coated with 10-kDa chondroitin sulfate achieved mouse survival rates of 100%, although that with hyaluronic acid did not.

Conclusions These findings suggest that GM-CSF/PEI coated with 10-kDa chondroitin sulfate has the potential for use in gene therapy of ovarian cancer.

Keywords cancer gene therapy; chondroitin sulfate; hyaluronic acid; ovarian cancer; polyethyleneimine; ternary plasmid complex: GM-CSF

Introduction

Although replication-competent viruses have been developed for treating cancers, their cytotoxic effects are insufficient because infection with them

is inhibited by the generation of neutralizing antibodies. A replication-competent virus-infected carrier cell overcomes virus-induced immunogenicity and induces complete tumor reduction [1]. This carrier cell system has asscociated problems, including difficulties of systemic administration as a result of trapping in capillary vessels, life-threatening serious side-effects as a result of replication-competent virus-induced cytokine surge, difficulties with mass industrial production, the need for liquid nitrogen for stocking, instability on long-term storage, and the need for hospitalization and an isolated room as a result of the biodiversity treaty. The development of a safe nonviral vector system is thus clearly required.

Polycations and cationic lipids electrostatically bind to DNA and facilitate gene transfer into target cells *in vitro*. *In vivo* transfection of this binary DNA/cation complex is difficult because the surfaces of the complexes are usually positively charged, and interaction with blood cells, serum proteins and extracellular matrix prevents their efficient delivery [2–4]. A protective polyanion coating was developed to afford negatively-charged DNA complexes [5], which exhibit diminished interaction with serum proteins.

Plasmid/polycation/polyanion ternary complexes have a negative surface charge and exhibit high dispersion stability, even in the presence of blood cells or proteins. Polyanions play roles not only in protective coating, but also as ligands for target cells [4,6] and transcriptional enhancers [6,7], and some degree of improvement in reporter-gene expression in tumor has been observed after their injection into the tail vein of mice [8,9]. Particles with a diameter < 100 nm are required for distribution in the body and accumulation in tumors as a result of enhanced permeability and retention. Mixing of DNA and polycations under highly concentrated conditions usually yields much larger particles (> 200 nm). Moreover, DNA/polycation binary complexes readily aggregate and thereby increase in size [10]. However, DNA/polycation/polyanion ternary complexes can be concentrated by freeze-drying and undergo rehydration without aggregation or inactivation [11].

Hyaluronic acid (HA) and chondroitin sulfate (CS), which are present in tumor matrix, and the receptors of which are CD44 and overexpressed in metastatic cancer tissue, have been mainly used as anionic components of ternary complexes in drug delivery systems for cancer treatment [12,13]. Plasmid-granulocyte macrophage-colony stimulating factor (GM-CSF)/polyethyleneimine (PEI)/HA ternary complex expresses the genes only in tumors and not in normal tissues, and significantly suppresses B16 tumor growth [11], although the antitumor activity of GM-CSF/PEI/CS ternary complex remained to be identified. In the present study, we compared raw materials and molecular weight fractions of CS as an anionic component of ternary complexes and compared the antitumor activity of GM-CSF/PEI/CS with that of GM-CSF/PEI/HA for ovarian cancer.

Materials and methods

Cell lines and culture conditions

Human ovarian adenocarcinoma HEY, OCC1 and OVCAR3 cells from Dr G. Mills (The University of Texas, MD Anderson Cancer Center, TX, USA), human ovarian clear cell carcinoma RMG-1 cells from Dr S. Nozawa (Keio University, Tokyo, Japan) and murine ovarian cancer (OVHM) cells from Dr H. Fujiwara (Osaka University, Osaka, Japan) were obtained. Normal human fibroblast F27 cells were established by Dr K. Hashimoto (Ehime University, Japan). Human ovarian teratocarcinoma PA-1 and murine fibroblast Lcl-1D cells were obtained from the Japanese Collection of Research Bioresources Cell Bank (Osaka, Japan). Murine fibroblast cells (NIH/3 T3) was obtained from Dr Tagawa (Chiba Cancer Institute, Chiba, Japan). Human amniotic stem cells (ASP) were obtained from Dr N. Sakuragawa (Bioresource Application Institute, Aichi, Japan).

Cells were maintained in a humidified 5% CO_2/95% air incubator at 37 °C. All cell lines except human amniotic stem cells were grown in RPMI medium supplemented with 10% fetal bovine serum. Human amniotic stem cells were grown in DMEM/F12 with 10% fetal bovine serum, 10 ng/ml human leukemia inhibitory factor, 10 ng/ml epidermal growth factor and 10 ng/ml basic fibroblast growth factor.

Reagents

HA sodium salt and CS were supplied by Seikagaku Corp. (Tokyo, Japan). Linear PEI 'MAX' (MW 40 000) was purchased from Polyscience, Inc. (Warrington, PA, USA). Green fluorescent protein (GFP)-coding plasmid with cytomegalovirus promoter was obtained from Clontech Laboratories, Inc. (Mountain View, CA, USA). Plasmid coding luciferase gene was constructed by subcloning the *HindIII/XbaI* firefly luciferase cDNA fragment from the pGL3-control vector (Promega, Madison, WI, USA) into the pcDNA3.1 vector (Invitrogen, Carlsbad, CA, USA). Plasmid coding murine granulocyte macrophage-colony-stimulating factor (mGM-CSF) was similarly produced with pcDNA3.1 vector and the gene isolated from mouse lymphocytes. They were amplified in Escherichia coli and purified with a Qiagen Plasmid Mega Kit (Tokyo, Japan). Cell culture lysis reagent and luciferase assay substrate were purchased from Promega. The protein assay kit was obtained from Bio-Rad Laboratories (Hercules, CA, USA).

Freeze-dried and rehydrated DNA complex

Typically, an aqueous solution of plasmid DNA (30 μl; 0.792 mg/ml) was mixed with linear PEI solution (30 μl; 2.3 mg/ml) and then with a solution

of HA (60 μl; 10 mg/ml) or CS (60 μl; 2.3 mg/ml) as previously described [11]. All the solutions were prepared in pure water. After being left to stand for 20 min, they were freeze-dried, and the resulting white spongy complexes were rehydrated with water or 5% glucose to [DNA] = 200 μg/ml.

ζ-Potential and size measurement

The freeze-dried complex containing 1 μg of DNA was rehydrated with water (200 μl). After 30 min, it was diluted with 800 μl of water and the ζ-potential and the size was measured with a particle analyser (Zetasizer Nano ZS, Malvern, UK).

In vitro transfection

OVHM cells were seeded onto 24-well plates at 5×10^4 cells per well, and cultured for 2 days. Lyophilized-and-rehydrated luciferase complex suspensions were prepared in phosphate-buffered saline (PBS) ([DNA] = 200 μg/ml). After 20 min, they were added to the cells (1 μg of plasmid per well). After an additional 20-h incubation at 37 °C, the cells were lysed, and transgene expression and protein content in the lysate were assessed with the corresponding assay kit.

Each cell line was seeded onto 24-well plates at 5×10^4 cells per well, and cultured for ≥ 2 days. Lyophilized-and-rehydrated plasmid-GFP complex suspensions were prepared in PBS ([DNA] = 200 μg/ml). After 20 min, they were added to the cells (1 μg of plasmid per well). Liposomal transfection was carried out using LF2000 reagent (Invitrogen). GFP-positive cells were counted with a fluorescence microscope (Axiovert 40; Carl Zeiss, Hallbergmoos, Germany) and the transfection efficiency was estimated.

Inhibition of subcutaneous ovarian tumor growth in syngeneic mice

To determine inhibition of syngeneic subcutaneous tumor growth, murine OVHM cells (1×10^6) were injected into the left posterior flank of female (C57BL/6 × C3H/He) F_1 mice (CLEA Japan Inc., Tokyo, Japan). Freeze-dried ternary complex of HA or CS was rehydrated with 500 μl of PBS for intratumoral injection. When the size of the subcutaneous tumor reached 5–8 mm in diameter, the resuspended complex containing 100 μg of the plasmid was injected intratumorally every day for 3 days. These animal studies were approved by the Ehime University Review Board.

Inhibition of intraperitoneal ovarian tumor growth in syngeneic mice

To simulate a clinical trial of gene therapy for ovarian cancer, the orthotopic intraperitoneal carcinomatosis model was used because ovarian cancer remains localized within the peritoneal cavity in a large proportion of patients, ultimately causing local morbidity and lethal complications. Murine OVHM cells (1×10^6) were injected into the abdominal cavity of female (C57BL/6 × C3H/He) F_1 mice (CLEA Japan Inc.). Freeze-dried ternary complex of HA or CS was rehydrated with 7 ml of PBS. Four to nine days after intraperitoneal inoculation of OVHM cells, the re-suspended and diluted complex containing 100 μg of plasmid was injected intraperitoneally and subcutaneously every day for 6 days. A 2-ml portion of 7 ml of ternary complex containing PBS was injected into the OVHM cell-injected abdominal skin to prevent local recurrence of OVHM tumor, and the remaining 5 ml of ternary complex containing PBS was injected into the peritoneal space because this subcutaneous injection prevents local recurrence, whereas no subcutaneous injection induced local recurrence in more than 80% of mice, and this excess amount of intraperitoneal injection could increase the antitumor activity of ternary complex. These animal studies were approved by the Ehime University Review Board.

Statistical analysis

Values are reported as the mean ± SD, and were examined with the unpaired *t*-test, Welch test and regression analysis. Survival data were plotted on Kaplan–Meier curves, and examined with the log-rank test using the LIFETEST procedure. $p < 0.05$ was considered statistically significant.

Results

Ten-kilodalton (kDa) CS yields efficient tumor-specific transfection

To obtain strong antitumor activity, high-molecular-weight (730 kDa) HA and the low-molecular-weight CS, which are present in tumor matrix and glycosaminoglycans, were compared as the anionic component of ternary DNA complex. In the ζ-potential assay, DNA and binary and ternary complexes were charged negatively, positively and negatively, respectively (Figure 1A). In the luciferase assay, luciferase activity of ternary complex with 10-kDa shark CS was three-fold higher than that of chicken HA and significantly higher than those of other higher-molecular-weight fractions of shark or cattle CS (Figure 1B). This 10-kDa shark CS was therefore used as an anionic component of ternary complex in this experiment. The size of DNA/PEI/CS was distributed from 59 to 164 nm, which is smaller than that of DNA/PEI/HA from 79 to 531, and the peak size of DNA/PEI/CS was 79 nm, which is 65% of that of DNA/PEI/HA at 122 nm (Figure 1C). Although binary GFP/PEI aggregated red blood cells (Figure 2A), ternary GFP/PEI/CS did not (Figure 2B). GFP plasmid yielded GFP-positive cells in none of the cell lines tested. LF2000 transfection and binary GFP/PEI did not yield significant differences in the numbers of GFP-positive cells between normal and cancer cells. The rate of transfection

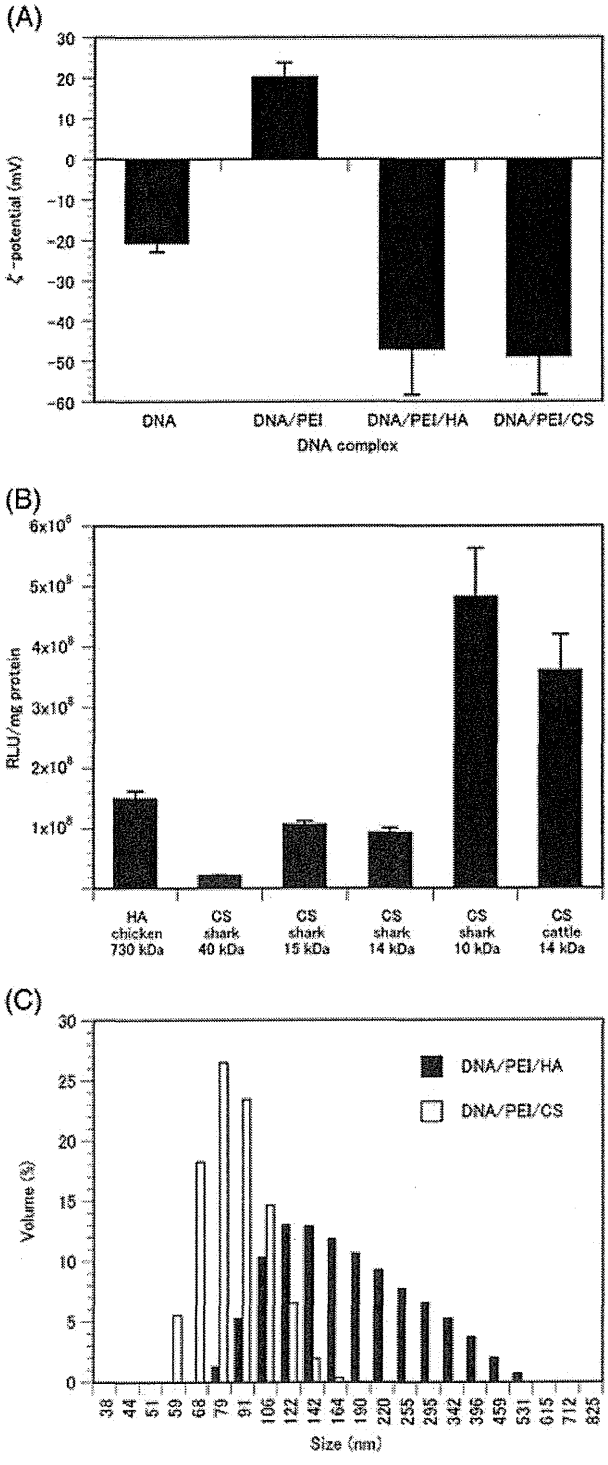

Figure 1. (A) ζ-potentials (mV) of DNA, binary DNA/PEI and ternary DNA/PEI/HA and CS complexes. (B) Luciferase activity of luciferase/PEI coated with HA from chicken and each molecular weight fraction of CS from shark or cow in cultured OVHM cells. RLU, relative light units. (C) The size of ternary DNA/PEI/HA and CS complexes.

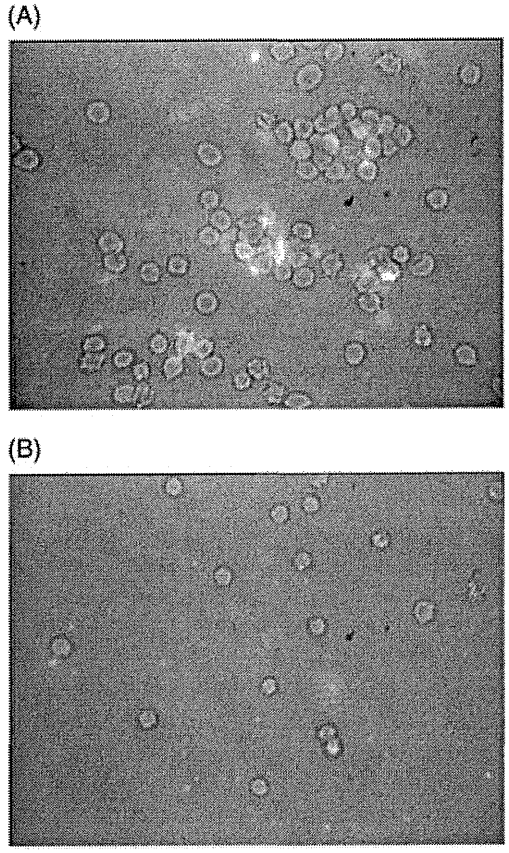

Figure 2. Binary GFP/PEI complex (A) and ternary GFP/PEI/CS complex (B) was incubated with red blood cells. Magnification: × 60.

with ternary GFP/PEI/HA or GFP/PEI/CS transfection in cancer cells was significantly higher than that in normal cells, and the rate of transfection with ternary GFP/PEI/CS transfection was significantly higher than that with GFP/PEI/HA transfection in all cancer cell lines examined (Figure 3A). LF2000 was highly toxic for all cell lines compared with binary and ternary complexes. Binary complex was more toxic than ternary complexes for all cell lines tested, except OVHM and ASP (Figure 3B). GFP expression by ternary GFP/PEI/CS or GFP/PEI/HA transfection peaked at days 2 or 3 and persisted for 9–27 days in cancer cells (Figure 4).

Antitumor effect of small mGM-CSF/PEI/CS ternary complex on subcutaneous tumor-bearing mice

Small DNA/PEI/HA or CS complexes were prepared with mGM-CSF-coding plasmid. It was freeze-dried and rehydrated at 200 μg/ml for intratumoral injection. Mice bearing OVHM tumor were injected with the complex three times daily (each injection, 100 μg/500 μl of plasmid per mouse). All control mice injected with medium died within 102 days. Binary mGM-CSG/PEI complex yielded a 20% rate of complete tumor reduction, whereas ternary mGM-CSF/PEI/HA complex and ternary mGM-CSF/PEI/CS complex yielded rates of 82% and 100%, respectively (Figure 5A). These rates of reductions were significantly different among types of treatment.

DOI: 10.1002/jgm

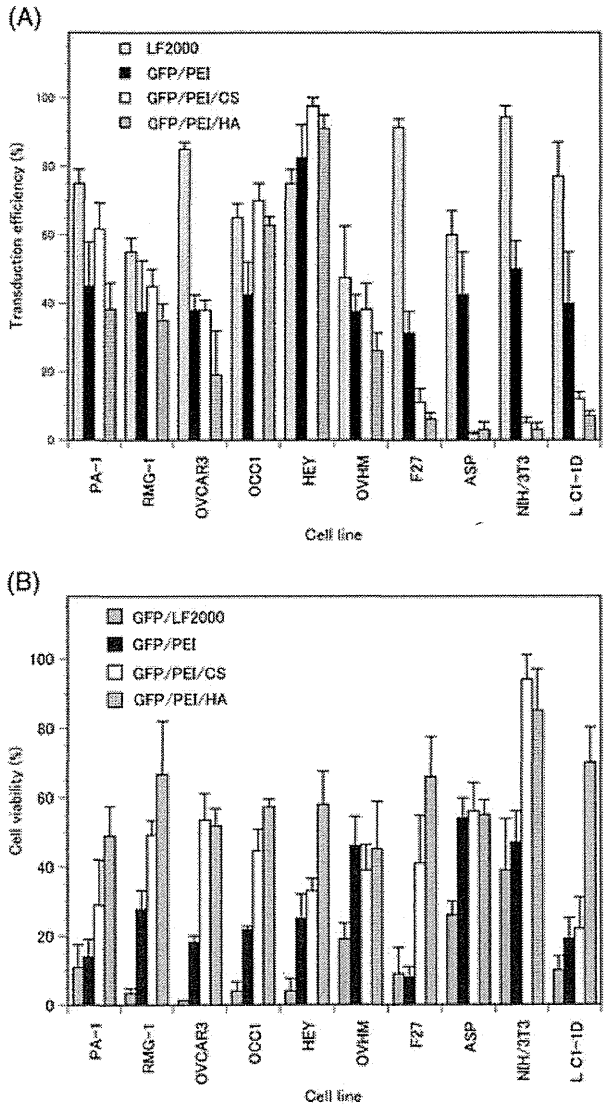

Figure 3. (A) Transfection efficiency of ternary GFP/PEI complex coated with HA or 10-kDa CS after 2 days of incubation. Percentage (%) of GFP-positive cells counted with a fluorescence microscope was considered transfection efficiency. (B) Viability of each cell line was determined by cell count assay after 2 days of incubation of LF2000-GFP, binary GFP/PEI complex, and ternary GFP/PEI complex coated with HA or 10-kDa CS.

Antitumor effect of small mGM-CSF/PEI/CS ternary complex on intraperitoneal tumor-bearing mice

Small DNA/PEI/HA or CS complexes were prepared with mGM-CSF-coding plasmid. It was freeze-dried, rehydrated and diluted in 7 ml of PBS for intraperitoneal and subcutaneous injection. Mice bearing intraperitoneal OVHM tumor were injected with the complex six times daily (each injection, 100 μg of the plasmid per mouse). All control mice injected with medium or binary mGM-CSG/PEI complex died within 31 and 28 days, respectively. Ternary mGM-CSF/PEI/HA complex significantly prolonged the survival of mice compared to mice injected with medium control or binary complex, although all mice died within 71 days. Furthermore, prolongation of survival was more pronounced with ternary mGM-CSF/PEI/CS complex than with mGM-CSF/PEI/HA, although all mice died within 130 days (Figure 5B).

Discussion

The numbers of deaths as a result of ovarian cancer in Japan and the USA are, respectively, 4000 and 14000 per year [14]. Of gynecologic cancers, ovarian cancer is the most important and has the poorest prognosis. Although the rate of recurrence of FIGO III stage ovarian cancer remains 60–70%, ovarian cancer in this stage of intraperitoneal carcinomatosis is curable because metastasis is local and within the abdominal cavity and not distant. Ovarian cancer readily metastasizes to the abdominal cavity because the ovaries abut the abdominal cavity. The present study demonstrated that ternary mGM-CSF/PEI/CS complex treatment significantly prolonged the survival of mice with intraperitoneal carcinomatosis treated with it despite a lack of complete remission, because 100 μg/500 μl of ternary complex is a concentration sufficient to treat 5–8 mm subcutaneous tumors but 100 μg/7 ml is not sufficient to treat tumors in the large intraperitoneal space. We set the upper limit of the dose at 600 μg/body considering safety with intraperitoneal administration because a greater than 1000 μg/body intraperitoneal injection of ternary complex induced 20–30% of mouse death, whereas less than 1000 μg/body that did not. It will be necessary to prolong the half-life of ternary DNA complex in the abdominal cavity because it readily migrates from the peritoneum to the systemic circulation and excess intraperitoneal doses of ternary DNA complex induce fatal side-effects as a result of PEI toxicity. A large amount of liquid solution, 5 ml of 7 ml, was used to treat intraperitoneal tumors because the 500 μl volume of liquid solution used for subcutaneous tumors cannot reach all of the intraperitoneal space. A 2 ml portion of 7 ml of ternary complex solution was injected into the OVHM cell-injected skin in the present study. This subcutaneous injection completely prevented the local recurrence of OVHM tumors in the injected skin because more than 80% of mice exhibited recurrence in the injected skin without any subcutaneous injection of ternary complex solution. It appears likely that the treatment with this ternary GM-CSF/PEI/CS complex only cannot achieve cure but may furthermore improve survival in cases of intraperitoneal ovarian carcinomatosis, together with anticancer agents such as taxols, cisplatin, and others.

GM-CSF, which has broad biological activity, was one of the first cytokines to be identified [15]. GM-CSF regulates the viability, proliferation, differentiation and function of hematopoietic progenitor cells at the same time as increasing the viability and function of dendritic cells, the differentiation and growth of dermal Langerhans cells, and the ability of antigen-presenting cells to capture

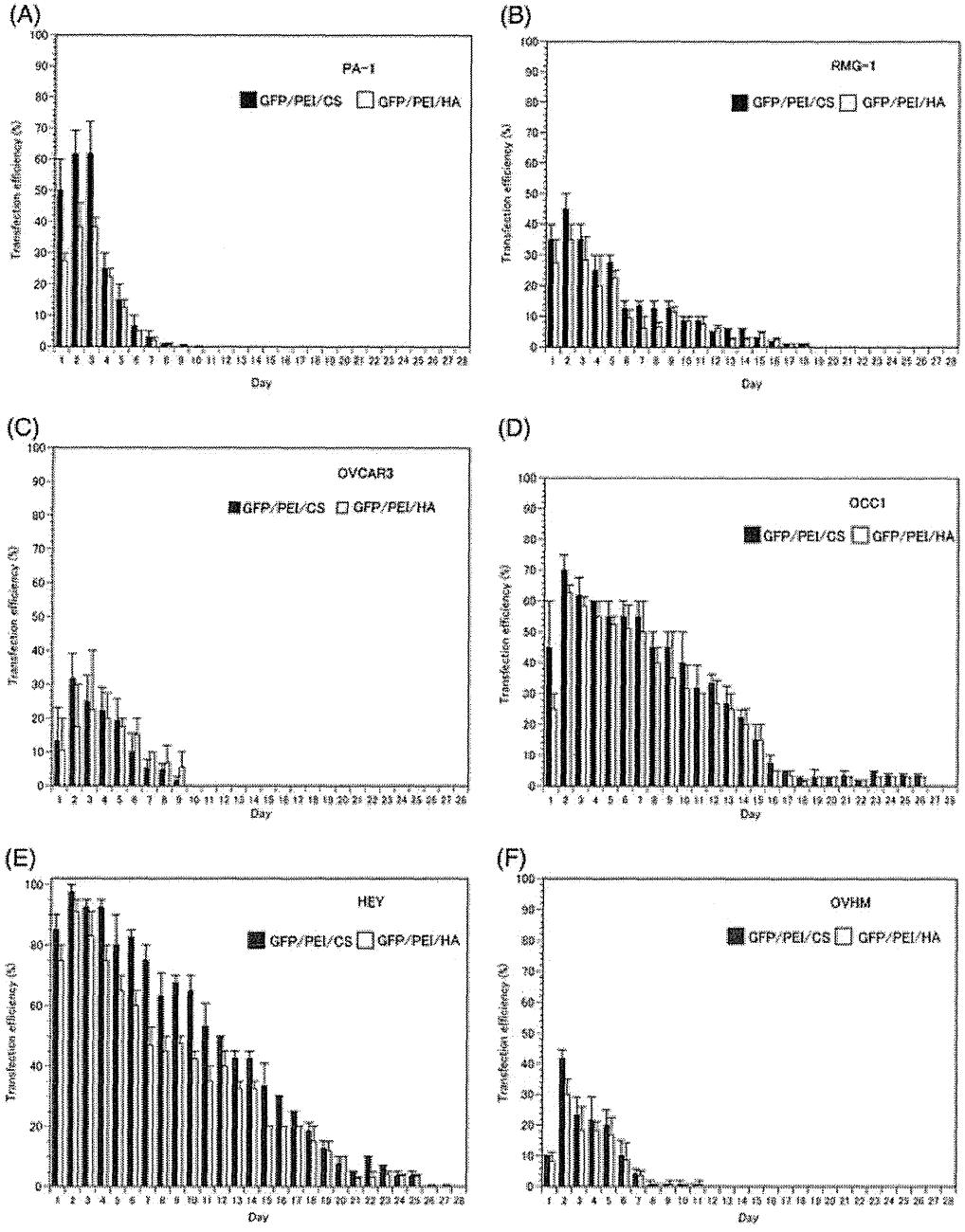

Figure 4. Time course of transfection efficiency of HA or 10-kDa CS in human ovarian carcinoma PA-1 (A), RMG-1 (B), OVCAR3 (C), OCC1 (D), HEY (E) and murine ovarian carcinoma OVHM (F) cells. Percentage (%) of GFP-positive cells was determined with a fluorescence microscope as the transfection efficiency.

foreign antigens [16]. GM-CSF alone or in combination with other cytokines has been reported to enhance immunity in cancer treatment [17,18]. Despite these pharmacological properties, GM-CSF has a very short biological half-life and therefore requires frequent injection throughout treatment, which results in problematic side-effects. In addition, the very limited serum stability of cytokines and easy destruction and inactivation of body proteins indicate the need for the investigation of new routes of administration of GM-CSF. We therefore investigated the efficacy of systems providing long durations of action in treatment with plasmid DNA coding GM-CSF.

Binary GM-CSF/chitosan and GM-CSF/PEI complexes were previously reported to induce immune responses to *Staphylococcus aureus* infection in dairy cattle [19] and to enhance antigen presentation in dendritic cell-based vaccination [17], respectively. Although ternary mGM-CSF/PEI/HA complex has been reported to inhibit the growth of mouse melanoma cell tumors [11], this has not yet been reported for ternary mGM-CSF/PEI/CS. We used a gene delivery system prepared with PEI in the

DOI: 10.1002/jgm